Colored five-vertex models and Demazure atoms

Ben Brubaker [a,*], Valentin Buciumas [b], Daniel Bump [c],
Henrik P.A. Gustafsson [c,d,e,f,1]

[a] *School of Mathematics, University of Minnesota, Minneapolis, MN 55455, United States of America*
[b] *School of Mathematics and Physics, The University of Queensland, St. Lucia, QLD, 4072, Australia*
[c] *Department of Mathematics, Stanford University, Stanford, CA 94305-2125, United States of America*
[d] *School of Mathematics, Institute for Advanced Study, Princeton, NJ 08540, United States of America*
[e] *Department of Mathematics, Rutgers University, Piscataway, NJ 08854, United States of America*
[f] *Department of Mathematical Sciences, University of Gothenburg and Chalmers University of Technology, SE-412 96 Gothenburg, Sweden*

A R T I C L E   I N F O

A B S T R A C T

Type A Demazure atoms are pieces of Schur functions, or sets of tableaux whose weights sum to such functions. Inspired by colored vertex models of Borodin and Wheeler, we will construct solvable lattice models whose partition functions are Demazure atoms; the proof of this makes use of a Yang-Baxter equation for a colored five-vertex model. As a byproduct, we will construct Demazure atoms on Kashiwara's $\mathcal{B}_\infty$ crystal and give new algorithms for computing Lascoux-Schützenberger keys.

© 2020 Elsevier Inc. All rights reserved.

* Corresponding author.
   E-mail addresses: brubaker@math.umn.edu (B. Brubaker), valentin.buciumas@gmail.com (V. Buciumas), bump@math.stanford.edu (D. Bump), gustafsson@ias.edu (H.P.A. Gustafsson).
[1] Until September 15, 2019: affiliation c. Since September 16, 2019: affiliations d, e, f.

1. Introduction

Exactly solvable lattice models have found numerous applications in the study of special functions. (See [38–41,25,26,55,37] to name but a few.) Here we use the Gelfand school interpretation of "special function," meaning one that arises as a matrix coefficient of a group representation. If the group is a complex Lie group or a p-adic reductive group, these matrix coefficients include highest weight characters and in particular, Schur polynomials, as well as Demazure characters and various specializations and limits of Macdonald polynomials. Many of these special functions may be studied by methods originating in statistical mechanics, by expressing them as a multivariate generating function (the "partition function") over the admissible states of a solvable lattice model. The term "solvable" means that the model possesses a solution of the Yang-Baxter equation that often permits one to express the partition function of the model in closed form. Knowing that a special function is expressible as a partition function of a solvable lattice model then leads to a host of interesting combinatorial properties, including branching rules, exchange relations under Hecke operators, Pieri- and Cauchy-type identities, and functional equations.

We will concentrate on the five- and six-vertex models on a square lattice, two-dimensional lattice models with five (respectively, six) admissible configurations on the edges adjacent to any vertex in the lattice. The latter models are sometimes referred to as "square ice" models, as the six configurations index the ways in which hydrogen atoms may be placed on two of the four edges adjacent to an oxygen atom at each vertex. Then weights for each configuration may be chosen so that the partition function records the probabilities that water molecules are arranged in various ways on the lattice (see for example [4]). More recently, lattice models with different weighting schemes have been studied in relation with certain stochastic models like the Asymmetric Simple Exclusion Process (ASEP) or the Kardar-Parisi-Zhang (KPZ) stochastic partial differential equation. These were shown to be part of a large family of solvable lattice models, called stochastic higher spin six-vertex models in [7,19]. Solutions to the Yang-Baxter equation also arise naturally from R-matrices of quantum groups; these higher spin models were associated to R-matrices for $U_q(\widehat{\mathfrak{sl}}_2)$. In this paper, we only make use of the associated quantum groups to differentiate among the various lattice model weighting schemes and the resulting solutions to the Yang-Baxter equations.

Subsequently, Borodin and Wheeler [9] introduced generalizations of the above models, which they call colored lattice models. Antecedents to these colored models appeared earlier in [8,23]. (A different notion of "colored" models appears in many other works such as [1].) In [9], "colors" are additional attributes introduced to the boundary data and internal edges of a given model, corresponding to replacing the governing quantum group $U_q(\widehat{\mathfrak{sl}}_2)$ in the setting mentioned above by $U_q(\widehat{\mathfrak{sl}}_{r+1})$. The partition functions of their colored lattice models are non-symmetric *spin* Hall-Littlewood polynomials. These are functions depending on a parameter s, which recover non-symmetric Hall-Littlewood polynomials when one sets $s = 0$.

The idea of introducing "color" in this way may be applied to a wide variety of lattice models. If one chooses the Boltzmann weights for the colored models appropriately, then one obtains a refinement of the (uncolored) partition function as a sum of partition functions indexed by all permutations of colors. Moreover, if the resulting colored model is solvable, then similar applications to those described above will follow. For example in [9], properties for these generalizations of Hall-Littlewood polynomials are proved including branching rules, exchange relations under Hecke divided-difference operators and Cauchy type identities motivated by the study of multi-species versions of the ASEP.

Inspired by these ideas of Borodin and Wheeler, this paper studies colored versions of an (uncolored) five-vertex model whose partition function is (up to a constant) a Schur polynomial s_λ indexed by a partition λ. The states of the uncolored system are in bijection with the set of semi-standard Young tableaux of shape λ, so the partition function may be evaluated using the combinatorial definition of the Schur function. This uncolored five-vertex model is a degeneration (crystal limit) of a six-vertex model described in Hamel and King [27], that is similarly equivalent to the generalization of the combinatorial definition of the Schur function by Tokuyama [53]. These models were shown to be solvable by Brubaker, Bump and Friedberg [12]. See Section 3 for the full definition of the uncolored five-vertex model used in this paper.

In Section 4 we introduce our colored five-vertex model. A color is assigned to each of the r rows of its rectangular lattice and permuting these colors gives a system for each element of the symmetric group S_r. We introduce Boltzmann weights for the colored models that simultaneously refine the uncolored model and produce a (colored) Yang-Baxter equation associated to a quantum superalgebra (see Theorem 4.2). This allows us to evaluate the partition functions for the colored models for each $w \in S_r$ and prove in Theorem 4.4 that they are *Demazure atoms* of Cartan Type A.

Demazure atoms, introduced by Lascoux and Schützenberger [42] and referred to as "standard bases" there, decompose Demazure characters into their smallest non-intersecting pieces. So in particular, summing Demazure atoms over a Bruhat interval produces Demazure characters. Mason [47] coined the term "atoms" and showed that they are specializations of non-symmetric Macdonald polynomials of Cartan Type A with $q = t = 0$. Basic properties of Demazure atoms and characters are reviewed in Section 2.

Demazure characters and Schur polynomials may be viewed as polynomial functions in formal variables or as functions on an algebraic torus associated to a given reductive group. But they may also be lifted to subsets of the Kashiwara-Nakashima [34] crystal $\mathcal{B}_\lambda$ whose elements are semistandard Young tableaux of a given shape λ, called *Demazure crystals*. The existence of such a lift of Demazure modules to crystals was shown by Littelmann [44] and Kashiwara [32]. Summing the weights of the Demazure crystal recovers the Demazure character.

Just as Littelmann and Kashiwara lifted Demazure characters to the crystal, polynomial Demazure atoms may also be lifted to subsets of the crystal. We will call these sets *crystal Demazure atoms*. Summing the weights of the crystal Demazure atom,

one obtains the usual polynomial Demazure atom. Crystals and the refined Demazure character formula are briefly reviewed in Section 5.

Although the theory of Demazure characters and crystals is in place for all Cartan types, most of the literature concerning Demazure atoms and the related topic of Lascoux-Schützenberger keys (including this paper) is for Cartan Type A. However the $\overline{B}_{w\lambda}(\lambda)$ in Section 9.1 of in [33] are Demazure atoms for crystals of symmetrizable Kac-Moody Cartan types. Moreover recently [29] (using the results in [33]) defined keys for all Kac-Moody Cartan types, with a special emphasis on affine Type A. There are also Type C results in [50]. See [28,2] for other recent work on Demazure atoms.

Based on Theorem 4.4, which shows that the partition functions of our colored models are Type A Demazure atoms, it is natural to ask for a more refined version of the connection between colored ice and the crystal Demazure atoms. In Section 6, we accomplish this by exhibiting a bijection between the admissible states of colored ice and crystal Demazure atoms as a subset of an associated crystal $\mathcal{B}_\lambda$. Showing this refined bijection is much more difficult than the initial evaluation of the partition function. Its proof forms a major part of this paper and builds on Theorem 5.5, which gives an algorithmic description of Demazure atoms. This result is proved in Section 8 after introducing Kashiwara's $\mathcal{B}_\infty$ crystal in Section 7. As a byproduct of our arguments, we will also obtain a theory of Demazure atoms on $\mathcal{B}_\infty$. The proofs take input from both the colored ice model and the Yang-Baxter equation, and from crystal base theory, particularly Kashiwara's $\star$-involution of $\mathcal{B}_\infty$.

Another byproduct of the results in Section 6 is a new formula for *Lascoux-Schützenberger keys* in Type A. These are tableaux with the defining property that each column (except the first) is a subset of the column before it. What is most important is that each crystal Demazure atom contains a unique key. Thus if $T \in \mathcal{B}_\lambda$ there is a unique key **key**(T) that is in the same crystal Demazure atom as T; this is called the *right key* of T. We will review this theory in Subsection 1.1. Algorithms for computing **key**(T) may be found in [42,49,43,47,46,56,48,57,58,3,51]. These papers are concerned with Type A Demazure atoms, but a few papers consider other Cartan types. Jacon and Lecouvey [29] (using the results in [33]) defined keys for all Kac-Moody Cartan types, with a special emphasis on affine Type A. There are also Type C results in [50]. See [28,2] for other recent work on Demazure atoms.

In this paper we give a new algorithm for computing the Lascoux-Schützenberger right key of a tableau in a highest weight crystal. Since this algorithm may be of independent interest we will describe it (and the topic of Lascoux-Schützenberger keys) in this introduction, in Subsection 1.1 below. We prove the algorithm in Section 9.

This paper also serves as a stepping stone to colored versions of the six-vertex (or "ice" type) models of [12] and of [10]. Indeed, since the results of this paper, we have shown that analogous colored partition functions recover special values of Iwahori fixed vectors in Whittaker models for general linear groups over a p-adic field [11] and their metaplectic covers (in progress), respectively. The colored five-vertex model in this paper is a degeneration of these models. Other recent developments (since this paper first

appeared) include applications of colored lattice models and the Yang-Baxter equation to Grothendieck and related polynomials [15,16,14]. See also Remark 4.5.

1.1. Lascoux-Schützenberger keys

Type A Demazure atoms are pieces of Schur functions: if λ is a partition of length $\leqslant r$, the Schur function $s_\lambda(z_1, \cdots, z_r)$ can be decomposed into a sum, over the Weyl group $W = S_r$, of such atoms. This is an outgrowth of the Demazure character formula: if ∂_w is the Demazure operator defined later in Section 2 then $\partial_w \mathbf{z}^\lambda$ is called a *Demazure character*. Originally these were introduced by Demazure and by Bernstein, Gelfand and Gelfand [20,6] to study the cohomology of line bundles on flag and Schubert varieties. A variant represents the Demazure character as $\sum_{y \leqslant w} \partial_y^\circ \mathbf{z}^\lambda$ where ∂_y° are modified operators, and $y \leqslant w$ is the Bruhat order. The components $\partial_y^\circ \mathbf{z}^\lambda$ are called (polynomial) *Demazure atoms.*

As we will explain in Section 4, a state of the colored lattice model features r colored lines running through a grid moving downward and rightward. These can cross, but they are allowed to cross at most once. Each line intersects the boundary of the grid in two places, and the colors are permuted depending on which lines cross. Hence they determine a permutation w from this braiding, which can be encoded into the boundary conditions. This allows us to construct a system $\mathfrak{S}_{\mathbf{z},\lambda,w}$ whose partition function satisfies the identity

$$Z(\mathfrak{S}_{\mathbf{z},\lambda,w}) = \mathbf{z}^\rho \partial_w^\circ \mathbf{z}^\lambda, \tag{1.1}$$

where ρ is the Weyl vector. Here the polynomial $\partial_w^\circ \mathbf{z}^\lambda$ is the Demazure atom.

The Schur function s_λ is the character of the Kashiwara-Nakashima [34] crystal $\mathcal{B}_\lambda$ of tableaux. The Demazure character formula was lifted by Littelmann [44] and Kashiwara [32] to define subsets $\mathcal{B}_\lambda(w) \subseteq \mathcal{B}_\lambda$ whose characters are Demazure characters $\partial_w \mathbf{z}^\lambda$. If $w = 1_W$ then $\mathcal{B}_\lambda(w) = \{v_\lambda\}$ where v_λ is the highest weight element. If w_0 is the long element then $\mathcal{B}_\lambda(w_0) = \mathcal{B}_\lambda$. If $w \leqslant w'$ in the Bruhat order then $\mathcal{B}_\lambda(w) \subseteq \mathcal{B}_\lambda(w')$.

In Type A, the results of Lascoux and Schützenberger [42] give an alternative decomposition of $\mathcal{B}_\lambda$ into disjoint subsets that we will here denote $\mathcal{B}_\lambda^\circ(w)$. Then

$$\mathcal{B}_\lambda(w) = \bigcup_{y \leqslant w} \mathcal{B}_\lambda^\circ(y).$$

The term *Demazure atom* is used in the literature to mean two closely related but different things: the sets that we are denoting $\mathcal{B}_\lambda^\circ(w)$ or their characters, which are the functions $\partial_w^\circ \mathbf{z}^\lambda$. When we need to distinguish them, we will use the term *crystal Demazure atoms* to refer to the subsets $\mathcal{B}_\lambda^\circ(w)$ while their characters will be referred to as *polynomial Demazure atoms.*

Since (up to the factor $\mathbf{z}^\rho$) the character of the colored system indexed by w is the polynomial Demazure atom $\mathcal{B}_\lambda^\circ(w)$, we may hope that, when we identify the set of states

of our model with a subset of $\mathcal{B}_\lambda$, the set of states indexed by w is $\mathcal{B}_\lambda^\circ(w)$. This is true and we will give a proof of this fact using techniques developed by Kashiwara, particularly the $\star$-involution of the $\mathcal{B}_\infty$ crystal, as well as (1.1), which is proved using the Yang-Baxter equation.

As a byproduct of this proof we obtain apparently new algorithms for computing Lascoux-Schützenberger right keys, which we now explain.

First, we will explain a theorem of Lascoux-Schützenberger that concerns the following question: given a tableau $T \in \mathcal{B}_\lambda$, determine $w \in W$ such that $T \in \mathcal{B}_\lambda^\circ(w)$. The set of Demazure atoms is in bijection with the orbit $W\lambda$ in the weight lattice, and this bijection may be made explicit as follows. The weights $W\lambda$ are extremal in the sense that they are the vertices of the convex hull of the set of weights of $\mathcal{B}_\lambda$. Each extremal weight $w\lambda$ has multiplicity one, in that there exists a unique element $u_{w\lambda}$ of $\mathcal{B}_\lambda$ with weight $w\lambda$. These extremal elements are called *key tableaux*, and they may be characterized by the following property: if $C_1, \ldots, C_k$ are the columns of a tableau T, then T is a key if and only if each column C_i contains C_{i+1} elementwise.

Lascoux and Schützenberger proved that every crystal Demazure atom contains a unique key tableau, and every key tableau is contained in a unique crystal Demazure atom. The weight of the key tableau in $\mathcal{B}_\lambda^\circ(w)$ is $w\lambda$. If $T \in \mathcal{B}_\lambda$ let $\mathbf{key}(T)$ be the unique key that is in the same atom as T. This is called the *right key* by Lascoux and Schützenberger; its origin is in the work of Ehresmann [22] on the topology of flag varieties. (There is also a *left key*, which is $\mathbf{key}(T')'$, where $T \mapsto T'$ is the Schützenberger (Lusztig) involution of $\mathcal{B}_\lambda$.)

We will describe two apparently new algorithms that compute $\mathbf{key}(T')$ and $\mathbf{key}(T)$, respectively. The algorithms depend on a map $\sigma : \mathcal{B}_\lambda \to W$ such that if $w = w_0\sigma(T)$ then $T \in \mathcal{B}_\lambda^\circ(w)$. Thus $\mathbf{key}(T)$ is determined by the condition that $\mathrm{wt}\big(\mathbf{key}(T)\big) = w\lambda = w_0\sigma(T)\lambda$. The extremal weight $w\lambda$ has multiplicity one in the crystal $\mathcal{B}_\lambda$, so the unique key tableau $\mathbf{key}(T)$ with that weight is determined by $w\lambda$. To compute it, the most frequently occurring entry (as specified by the weight) must appear in every column of $\mathbf{key}(T)$, the next most frequently occurring entry must then appear in every remaining, non-filled column, and so on. The entries of the columns are thus determined, and arranging each column in ascending order we get $\mathbf{key}(T)$.

A formal definition of the map σ will be given later in (5.11). But we will now give two algorithms for computing it. Given a tableau T, the first algorithm computes $\sigma(T')$, and the second algorithm computes $\sigma(T)$. The two algorithms depend on the notion of a *nondescending product* of a sequence of simple reflections s_i in the Weyl group W. Let $i_1, \cdots, i_k$ be a sequence of indices and define the *nondescending product* $\Pi_{\mathrm{nd}}(s_{i_1}, \cdots, s_{i_k})$ to be s_{i_1} if $k = 1$ and then recursively

$$\Pi_{\mathrm{nd}}(s_{i_1}, \cdots, s_{i_k}) = \begin{cases} s_{i_1}\pi & \text{if } s_{i_1}\pi > \pi \\ \pi & \text{otherwise,} \end{cases} \tag{1.2}$$

where $\pi = \Pi_{\mathrm{nd}}(s_{i_2}, \cdots, s_{i_k})$.

Remark 1.1. There is another way of calculating the nondescending product. There is a degenerate Hecke algebra $\mathcal{H}$ with generators S_i subject to the braid relations and the quadratic relation $S_i^2 = S_i$.[2] Given $w \in W$, set $S_w = S_{j_1} \cdots S_{j_\ell}$ where $w = s_{j_1} \cdots s_{j_\ell}$ is a reduced expression. Then the S_w ($w \in W$) form a basis of $\mathcal{H}$, and we will denote by $\{\cdot\}$ the map from this basis to W that sends S_w to w. Then

$$\Pi_{\mathrm{nd}}(s_{i_1}, \cdots, s_{i_k}) = \{S_{i_1} \cdots S_{i_k}\} .$$

An element T of $\mathcal{B}_\lambda$ is a semistandard Young tableau with entries in $\{1, 2, \ldots, r\}$ and shape λ. There is associated with T a Gelfand-Tsetlin pattern $\Gamma(T)$ as follows. The top row is the shape λ; the second row is the shape of the tableau obtained from T by erasing all entries equal to r. The third row is the shape of the tableau obtained by further erasing all $r-1$ entries, and so forth. For example suppose that $r = 4$, $\lambda = (5, 3, 1)$. Here is a tableau and its Gelfand-Tsetlin pattern:

$$T = \begin{array}{|c|c|c|c|c|}\hline 1 & 1 & 2 & 4 & 4 \\\hline 2 & 3 & 4 \\\cline{1-3} 3 \\\cline{1-1}\end{array}, \qquad \Gamma(T) = \left\{\begin{array}{ccccccc} 5 && 3 && 1 && 0 \\ & 3 && 2 && 1 & \\ && 3 && 1 && \\ &&& 2 &&& \end{array}\right\}. \qquad (1.3)$$

First algorithm

To compute $\sigma(T')$, we decorate the Gelfand-Tsetlin pattern as follows. For each subtriangle

$$\begin{array}{ccc} x && y \\ & z & \end{array}$$

if $z = y$ then we circle the z. We then transfer the circles in the Gelfand-Tsetlin pattern to the following array:

$$\begin{bmatrix} s_1 & & s_2 & & \cdots & & s_{r-1} \\ & \ddots & & \vdots & & \cdot^{\cdot^{\cdot}} & \\ & & s_1 & & s_2 & & \\ & & & s_1 & & & \end{bmatrix}. \qquad (1.4)$$

Note that the array of reflections has one fewer row than the first, but that circling cannot happen in the top row of the Gelfand-Tsetlin pattern. Now we traverse this array in the order bottom to top, right to left. We take the subsequence of circled entries in the indicated order, and their nondescending product is $\sigma(T')$.

---

[2] It may be worth remarking that these are the same relations satisfied by the Demazure operators ∂_i.

Second algorithm

To compute $\sigma(T)$, we decorate the Gelfand-Tsetlin pattern as follows. For each subtriangle

$$x \qquad y$$
$$z$$

if $z = x$ then we circle the z. We then transfer the circles in the Gelfand-Tsetlin pattern to the following array:

$$\begin{bmatrix} s_1 & & s_2 & & \cdots & & s_{r-1} \\ & \ddots & & & \vdots & & & \ddots \\ & & s_{r-2} & & & s_{r-1} & \\ & & & s_{r-1} & & & \end{bmatrix}. \tag{1.5}$$

Now we traverse this array in the order bottom to top, left to right. We take the subsequence of circled entries in the indicated order, and their nondescending product is $\sigma(T)$.

Let us illustrate these algorithms with the example (1.3).

For the first algorithm, we obtain the following circled Gelfand-Tsetlin pattern and array of simple reflections

$$\left\{ \begin{matrix} 5 & & 3 & & 1 & & 0 \\ & ③ & & 2 & & 1 & \\ & & 3 & & ① & \\ & & & 2 & & \end{matrix} \right\}, \qquad \begin{bmatrix} ⓢ_1 & & s_2 & & s_3 \\ & s_1 & & ⓢ_2 & \\ & & s_1 & & \end{bmatrix}$$

The first algorithm predicts that if T' is the Schützenberger involute of T then $\sigma(T') = s_2 s_1$, which is the nondescending product of the circle entries in the order bottom to top, right to left. Thus $w_0 \sigma(T') = w_0 s_2 s_1 = s_1 s_2 s_3 s_2$. We claim that $\mathbf{key}(T')$ is the unique key tableau with shape $(5, 3, 1, 0)$ having weight $w_0 \sigma(T')\lambda = (0, 5, 1, 3)$. Let us check this. The tableau T' and its key (computed by Sage using the algorithm in Willis [57]) are:

$$T' = \begin{array}{|c|c|c|c|c|} \hline 1 & 1 & 1 & 2 & 2 \\ \hline 3 & 3 & 4 \\ \cline{1-3} 4 \\ \cline{1-1} \end{array}, \qquad \mathbf{key}(T') = \begin{array}{|c|c|c|c|c|} \hline 2 & 2 & 2 & 2 & 2 \\ \hline 3 & 4 & 4 \\ \cline{1-3} 4 \\ \cline{1-1} \end{array}.$$

As claimed $\mathrm{wt}(\mathbf{key}(T')) = w_0 \sigma(T')\lambda$.

For the second algorithm, there are two circled entries, and we transfer the circles to the array of reflections as follows:

$$\left\{ \begin{matrix} 5 & & 3 & & 1 & & 0 \\ & 3 & & 2 & & \textcircled{1} & \\ & & \textcircled{3} & & 1 & & \\ & & & 2 & & & \end{matrix} \right\} , \qquad \left[\begin{matrix} s_1 & & s_2 & & \textcircled{s_3} \\ & \textcircled{s_2} & & s_3 & \\ & & s_3 & & \end{matrix} \right]$$

Thus $\sigma(T) = s_2 s_3$ is the (nondescending) product in the order bottom to top, left to right. Then if $w = w_0 s_2 s_3 = s_3 s_1 s_2 s_1$, the right key of T is determined by the condition that its weight is $w\lambda = (1, 3, 0, 5)$. Indeed, the right key of T is

$$\mathbf{key}(T) = \begin{array}{|c|c|c|c|c|} \hline 1 & 2 & 2 & 4 & 4 \\ \hline 2 & 4 & 4 \\ \cline{1-3} 4 \\ \cline{1-1} \end{array} .$$

This is the unique key tableau with shape $(5, 3, 1, 0)$ and weight $(1, 3, 0, 5)$.

The two algorithms hinge on Theorem 5.5, which refines results on keys due to Lascoux and Schützenberger [42]. The proof of Theorem 5.5 is detailed in the subsequent three sections of the paper, and the resulting algorithms are proved in Section 9.

1.2. A sketch of the proofs

In Section 3 we review the *Tokuyama model* (in its crystal limit), a statistical-mechanical system $\mathfrak{S}_{\mathbf{z},\lambda}$ whose partition function is $\mathbf{z}^\rho s_\lambda(\mathbf{z})$ in terms of the Schur function s_λ (Proposition 3.2). The states of this 5-vertex model system are in bijection with $\mathcal{B}_\lambda$. For $w \in W$ we will describe a refinement $\mathfrak{S}_{\mathbf{z},\lambda,w}$ of this system in Section 4 whose states are a subset of those of $\mathfrak{S}_{\mathbf{z},\lambda}$. The Weyl group element w is encoded in the boundary conditions. Thus the set of states of $\mathfrak{S}_{\mathbf{z},\lambda,w}$ may be identified with a subset of $\mathcal{B}_\lambda$. If S is a subset of a crystal, the *character* of S is $\sum_{v \in S} \mathbf{z}^{\mathrm{wt}(v)}$. Using a Yang-Baxter equation, in Theorem 4.4, we are able to prove a recursion formula for the character of $\mathfrak{S}_{\mathbf{z},\lambda,w}$, regarded as a subset of $\mathcal{B}_\lambda$, and this is the same as the character of the crystal Demazure atom $\mathcal{B}_\lambda^\circ(w)$. This suggests but does not prove that the states of $\mathfrak{S}_{\mathbf{z},\lambda,w}$ comprise $\mathcal{B}_\lambda^\circ(w)$. The equality of $\mathfrak{S}_{\mathbf{z},\lambda,w}$ and $\mathcal{B}_\lambda^\circ(w)$ is Theorem 5.5. Leveraging the information in Theorem 4.4 into a proof of Theorem 5.5 is accomplished in Sections 7 and 8 using methods of Kashiwara [32], namely transferring the problem to the infinite $\mathcal{B}_\infty$ crystal, then using Kashiwara's $\star$-involution of that crystal to transform and solve the problem. The information that we obtained from the Yang-Baxter equation in Theorem 4.4 is used at a key step (8.3) in the proof. A more detailed outline of these proofs will be given near the beginning of Section 7.

The two algorithms are treated in Section 9, but the key insight is earlier in Theorem 6.1, where the first algorithm is proved for $\mathfrak{S}_{\mathbf{z},\lambda,w}$. The idea is that the unique permutation w such that a given state of $\mathfrak{S}_{\mathbf{z},\lambda}$ lies in of $\mathfrak{S}_{\mathbf{z},\lambda,w}$ is determined by the pattern of crossings of colored lines; these crossings correspond to the circled entries in

(1.4). Then with Theorem 5.5 in hand, the result applies to $\mathcal{B}_\lambda^\circ(w)$. The second algorithm is deduced from the first using properties of crystal involutions.

2. Demazure operators

This section reviews the theory of Demazure operators associated to any complex reductive Lie group G. Though most of the applications in the later sections will require only the results in Cartan Type A, it is natural to explain the theory using root datum for any such G. Let Φ be a root system with weight lattice Λ, which may be regarded as the weight lattice of G. Thus if T is a maximal torus of G, then we may identify Λ with the group $X^*(T)$ of rational characters of T. If $\mathbf{z} \in T$ and $\lambda \in \Lambda$ we will denote by $\mathbf{z}^\lambda$ the application of λ to $\mathbf{z}$. Let $\mathcal{O}(T)$ be the set of polynomial functions on T, that is, finite linear combinations of the functions $\mathbf{z}^\lambda$.

We decompose Φ into positive and negative roots, and let α_i ($i \in I$) be the simple positive roots, where I is an index set. Let $\alpha_i^\vee \in X_*(T)$ denote the corresponding simple coroots and s_i the corresponding simple reflections generating the Weyl group W. To each simple reflection s_i with $i \in I$, we define the isobaric Demazure operator acting on $f \in \mathcal{O}(T)$ by

$$\partial_i f(\mathbf{z}) = \frac{f(\mathbf{z}) - \mathbf{z}^{-\alpha_i} f(s_i \mathbf{z})}{1 - \mathbf{z}^{-\alpha_i}}. \tag{2.1}$$

The numerator is divisible by the denominator, so the resulting function is again in $\mathcal{O}(T)$.

It is straightforward to check that $\partial_i^2 = \partial_i = s_i \partial_i$. Given any $\mu \in \Lambda$, set $k = \langle \mu, \alpha_i^\vee \rangle$ so $s_i(\mu) = \mu - k\alpha_i$. Then the action on the monomial $\mathbf{z}^\mu$ is given by

$$\partial_i \mathbf{z}^\mu = \begin{cases} \mathbf{z}^\mu + \mathbf{z}^{\mu - \alpha_i} + \ldots + \mathbf{z}^{s_i(\mu)} & \text{if } k \geqslant 0, \\ 0 & \text{if } k = -1, \\ -(\mathbf{z}^{\mu + \alpha_i} + \mathbf{z}^{\mu + 2\alpha_i} + \ldots + \mathbf{z}^{s_i(\mu + \alpha_i)}) & \text{if } k < -1. \end{cases} \tag{2.2}$$

We will also make use of $\partial_i^\circ := \partial_i - 1$, that is

$$\partial_i^\circ f(\mathbf{z}) := \frac{f(\mathbf{z}) - f(s_i \mathbf{z})}{\mathbf{z}_i^\alpha - 1}.$$

Both ∂_i and ∂_i° satisfy the braid relations. Thus

$$\partial_i \partial_j \partial_i \cdots = \partial_j \partial_i \partial_j \cdots \, ,$$

where the number of terms on both sides is the order of $s_i s_j$ in W, and similarly for the ∂_i°. These are proved in [17], Proposition 25.1 and Proposition 25.3. (There is a typo in the second Proposition where the wrong font is used for ∂_i.) Consequently to each $w \in W$, and any reduced decomposition $w = s_{i_1} \cdots s_{i_k}$, we may define $\partial_w = \partial_{i_1} \cdots \partial_{i_k}$ and $\partial_w^\circ = \partial_{i_1}^\circ \cdots \partial_{i_k}^\circ$. For $w = 1$ we let $\partial_1 = \partial_1^\circ = 1$.

Let w_0 be the long Weyl group element. If λ is a dominant weight let χ_λ denote the character of the irreducible representation π_λ with highest weight λ. The *Demazure character formula* is the identity, for $\mathbf{z} \in T$:

$$\chi_\lambda(\mathbf{z}) = \partial_{w_0} \mathbf{z}^\lambda.$$

For a proof, see [17], Theorem 25.3. More generally for any Weyl group element w, we may consider $\partial_w \mathbf{z}^\lambda$. These polynomials are called *Demazure characters*.

Next we review the theory of (polynomial) *Demazure atoms*. These are polynomials of the form $\partial_w^\circ \mathbf{z}^\lambda$. They were introduced in Type A by Lascoux and Schützenberger [42], who called them "standard bases." The modern term "Demazure atom" was introduced by Mason in [47], who showed that they are specializations of nonsymmetric Macdonald polynomials, among other things. The following theorem, done for Type A in [42], relates Demazure characters and Demazure atoms and is valid for any finite Cartan type.

Theorem 2.1. *Let $f \in \mathcal{O}(T)$. Then*

$$\partial_w f(\mathbf{z}) = \sum_{y \leqslant w} \partial_y^\circ f(\mathbf{z}). \tag{2.3}$$

Proof. We prove this by induction with respect to the Bruhat order. Setting $\phi(w) := \partial_w^\circ f(\mathbf{z})$ and assuming the theorem for w, we must show that for any s_i with $s_i w > w$ in the Bruhat order,

$$\sum_{y \leqslant s_i w} \phi(y) = \partial_{s_i w} f(\mathbf{z}). \tag{2.4}$$

We recall "Property Z" of Deodhar [21], which asserts that if $s_i w > w$ and $s_i y > y$ then the following inequalities are equivalent:

$$y \leqslant w \quad \Longleftrightarrow \quad y \leqslant s_i w \quad \Longleftrightarrow \quad s_i y \leqslant s_i w \, .$$

Using this fact we may split the sum on the left-hand side as follows

$$\sum_{y \leqslant s_i w} \phi(y) = \sum_{\substack{y \leqslant s_i w \\ y < s_i y}} \phi(y) + \sum_{\substack{y \leqslant s_i w \\ s_i y < y}} \phi(y) = \sum_{\substack{y \leqslant s_i w \\ y < s_i y}} \phi(y) + \sum_{\substack{s_i y \leqslant s_i w \\ y < s_i y}} \phi(s_i y) = \sum_{\substack{y \leqslant w \\ y < s_i y}} \big(\phi(y) + \phi(s_i y) \big) \,.$$

If $s_i w > w$ then

$$\phi(w) + \phi(s_i w) = \partial_i \phi(w). \tag{2.5}$$

Indeed, since $\partial_i = \partial_i^\circ + 1$, this is another way of writing

$$\partial_{s_i w}^\circ f(\mathbf{z}) = \partial_i^\circ \partial_w^\circ f(\mathbf{z}) \,,$$

which follows from the definitions.

Using (2.5), we obtain

$$\sum_{y \leqslant s_i w} \phi(y) = \partial_i \Big(\sum_{\substack{y \leqslant w \\ y < s_i y}} \phi(y) \Big). \tag{2.6}$$

Still assuming $s_i w > w$ we will prove that

$$\partial_i \sum_{\substack{y \leqslant w \\ y < s_i y}} \phi(y) = \partial_i \sum_{y \leqslant w} \phi(y). \tag{2.7}$$

We split the terms on the right-hand side into three groups and write

$$\partial_i \sum_{y \leqslant w} \phi(y) = \partial_i \sum_{\substack{y \leqslant w \\ y < s_i y \\ s_i y \leqslant w}} \big(\phi(y) + \phi(s_i y) \big) + \partial_i \sum_{\substack{y \leqslant w \\ y < s_i y \\ s_i y \not\leqslant w}} \phi(y).$$

Now using (2.5) again this equals

$$\partial_i \sum_{\substack{y \leqslant w \\ y < s_i y \\ s_i y \leqslant w}} \partial_i \phi(y) + \partial_i \sum_{\substack{y \leqslant w \\ y < s_i y \\ s_i y \not\leqslant w}} \phi(y),$$

and remembering that $\partial_i^2 = \partial_i$ this equals

$$\partial_i \Big(\sum_{\substack{y \leqslant w \\ y < s_i y \\ s_i y \leqslant w}} \phi(y) + \sum_{\substack{y \leqslant w \\ y < s_i y \\ s_i y \not\leqslant w}} \phi(y) \Big) = \partial_i \sum_{\substack{y \leqslant w \\ y < s_i y}} \phi(y),$$

proving (2.7).

Now (2.4) follows using (2.6), (2.7) and our induction hypothesis. □

3. Ice models for $\mathbf{GL}(r)$

In statistical mechanics, an *ensemble* is a probability distribution over every possible admissible state (i.e., microscopic arrangement) of particles in a given physical system. The probability of any given state is measured by its *Boltzmann weight*, which is calculated by computing the energy associated to all local interactions between particles. If there are only finitely many admissible states in the ensemble (as in all of the examples in this paper), then the *partition function* is defined to be a sum of the Boltzmann weights of each state. While computing the partition function explicitly is often intractable, there is a nice class of so-called *solvable models* [4,30] for which the partition function may be computed using a microscopic symmetry of the partition function known as the *Yang-Baxter equation*. With few exceptions, solvable models are based on two-dimensional physical systems.

Ice-type models, including the *six-vertex* model and the *five-vertex* model, are a class of two-dimensional solvable models based on a square, planar grid in which admissible states are determined by associating one of two spins $\{+, -\}$ to each edge. See Fig. 1 for an example. The term *six-vertex* refers to the fact that only six admissible configurations of spins are allowed on the four edges adjacent to any vertex in the grid. Similarly, *five-vertex* models are systems, typically degenerations of six-vertex models, in which only five local configurations are allowed. An example of such a set of configurations can be found in Fig. 2 where the configuration labeled $\mathtt{b_1}$ is removed. In the next two sections, we will revisit all of the above terms and give precise definitions for an ensemble of admissible states and associated weights that result in a solvable model first for a five-vertex model based on the configurations in Fig. 2, and then generalizations thereof. Our Boltzmann weights for states will depend on several complex variables and while they will not try to model the probability distribution of a physical system, they will nonetheless result in solvable variants of the above five-vertex model whose partition functions are explicitly evaluable as Demazure atoms.

More precisely, inspired by colored lattice models in Borodin and Wheeler [9], we will show that Demazure atoms and characters for $\mathrm{GL}(r)$ can be represented as partition functions of certain "colored five-vertex models." Strictly speaking, it is no longer true that there are only five allowed configurations at a vertex. Still, the allowed configurations can be classified into five different groups, which we will denote $\mathtt{a_1}$, $\mathtt{a_2}$, $\mathtt{b_2}$, $\mathtt{c_1}$ and $\mathtt{c_2}$ in keeping with notational conventions of [4]. Before introducing the colored models, we begin with a model that is not new, but rather a special case of models due to Hamel and King [27] and Brubaker, Bump and Friedberg [12].

Our five-vertex models will occur on square grids inside a finite rectangle of fixed size. Then to describe the ensemble of admissible states of the model, it suffices to specify the size of the rectangle and the spins associated to edges along the boundary of this rectangle. Indeed, then the admissible states will consist of all possible assignments of spins to the remaining edges of the grid so that every vertex has adjacent edges in one of the five allowable configurations of Fig. 2 (those not of form $\mathtt{b_1}$).
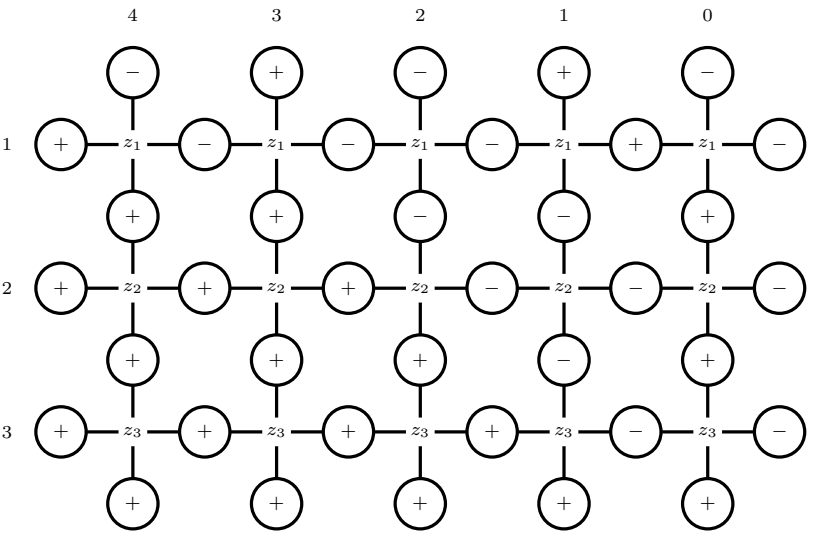
Fig. 1. A state of a five-vertex model system with $N = 4$, $r = 3$ and $\lambda = (2, 1, 0)$.

Fig. 2. Boltzmann weights $\mathrm{wt}(v)$ for a vertex v in the i-th row of the uncolored system.

Given an integer partition $\lambda = (\lambda_1, \ldots, \lambda_r)$ with r parts, our grid will have r rows and $N + 1$ columns, where N is a fixed integer at least $\lambda_1 + r - 1$. In order to enumerate the vertices, the columns are labeled 0 to N from right to left, and the rows are labeled 1 to r from top to bottom. Vertices occur at every crossing of rows and columns and boundary edges are those edges in the grid connected to only one vertex. The spins $\{+, -\}$ of the edges on the boundary are fixed according to the choice of λ by the following rules. For the top boundary edges, we put $-$ in the columns labeled $\lambda_i + r - i$ for $i \in \{1, \ldots, r\}$ and $+$ in the remaining columns. Then, we put $+$ on all the left and bottom boundary edges and $-$ on the right boundary edges. As noted above, an (admissible) *state* $\mathfrak{s}$ of the resulting system assigns spins to the interior edges so that each vertex is one of the five configurations in Fig. 2 *excluding* patterns of type $\mathsf{b_1}$, which are not allowed (or

equivalently, are assigned weight 0). An example of an admissible state for $\lambda = (2, 1, 0)$ and $N = 4$ is given in Fig. 1.

Next we describe the Boltzmann weight $\beta(\mathfrak{s})$ of a state $\mathfrak{s}$. It will depend on a choice of r complex numbers $\mathbf{z} = (z_1, \ldots, z_r)$ in $(\mathbb{C}^\times)^r$. We set

$$\beta(\mathfrak{s}) := \prod_{v: \text{ vertex in } \mathfrak{s}} \text{wt}(v),$$

where the function $\text{wt}(v)$ is defined in Fig. 2; the display of the variable z_i in the middle of a configuration is a reminder that the weight of a configuration is a function of the row in which it appears. For example, one may quickly check that the state in Fig. 1 has Boltzmann weight $z_1^3 z_2^2 z_3$.

Let $\mathfrak{S}_{\mathbf{z},\lambda}$ denote the ensemble of all admissible states with boundary conditions dictated by λ and weights depending on parameters $\mathbf{z} = (z_1, \ldots, z_r)$. Further define the *partition function* $Z(\mathfrak{S}_{\mathbf{z},\lambda})$ to be the sum of the Boltzmann weights over all states in the ensemble. Our notation suppresses the choice of number of columns N; indeed, the partition function is independent of any such (large enough) choice, since adding columns to the left of the $\lambda_1 + r - 1$ column adds only $\mathsf{a_1}$ patterns, which have weight 1.

We will next describe bijections between states of this system and two other sets of combinatorial objects: Gelfand-Tsetlin patterns with top row λ and semistandard Young tableaux of shape λ with entries in $\{1, 2, \ldots, r\}$. These will allow us to conclude that $Z(\mathfrak{S}_{\mathbf{z},\lambda})$ is, up to a simple factor, the Schur polynomial $s_\lambda(\mathbf{z})$.

Our boundary conditions imply via a combinatorial argument ([4] Section 8.3 or Proposition 19.1 in [13]) that in any given state $\mathfrak{s}$ of the system, the number of $-$ spins on the $N + 1$ vertical edges between row $i - 1$ and row i will be exactly $r + 1 - i$. Let (i, j) with $r \geqslant j \geqslant i$ enumerate these spins and let $A_{i,j}$ be their corresponding column numbers, in descending order. Then

$$\text{GTP}(\mathfrak{s}) := \left\{ \begin{matrix} A_{1,1} & & A_{1,2} & & \cdots & & A_{1,r} \\ & A_{2,2} & & \cdots & & A_{2,r} & \\ & & \ddots & & \vdots & \cdot^{\cdot^{\cdot}} & \\ & & & A_{r,r} & & & \end{matrix} \right\}$$

is a *left-strict* Gelfand-Tsetlin pattern, meaning that $A_{i,j} > A_{i+1,j+1} \geqslant A_{i,j+1}$. This follows from Proposition 19.1 of [13], taking into account the omission of $\mathsf{b_1}$ patterns in Fig. 2, which implies that the inequality $A_{i,j} > A_{i+1,j+1}$ is strict.

Remark 3.1. If we allowed patterns of type $\mathsf{b_1}$ we would have $A_{i,j} \geqslant A_{i+1,j+1} \geqslant A_{i,j+1}$ and $A_{i,j} > A_{i,j+1}$.

Since $\text{GTP}(\mathfrak{s})$ is left-strict, we may subtract $\rho_{r+1-i} := (r - i, r - i - 1, \cdots, 0)$ from the i-th row of $\text{GTP}(\mathfrak{s})$ to obtain another Gelfand-Tsetlin pattern. We denote this *reduced* pattern by

$$\text{GTP}^\circ(\mathfrak{s}) := \left\{ \begin{matrix} a_{1,1} & & a_{1,2} & & \cdots & & a_{1,r} \\ & a_{2,2} & & \cdots & & a_{2,r} & \\ & & \ddots & & \vdots & & \cdot^{\cdot^{\cdot}} \\ & & & a_{r,r} & & & \end{matrix} \right\}, \tag{3.1}$$

whose entries are $a_{i,j} = A_{i,j} - r + j$. The top row of $\text{GTP}^\circ(\mathfrak{s})$ is λ. The map $\mathfrak{s} \mapsto \text{GTP}^\circ(\mathfrak{s})$ is easily seen to be a bijection between the states of $\mathfrak{S}_{\mathbf{z},\lambda}$ and the set of Gelfand-Tsetlin patterns with top row λ.

There is also associated with a state $\mathfrak{s}$ a semistandard Young tableau, which may be described as follows. Let $\mathcal{B}_\lambda$ be the set of semi-standard Young tableaux of shape λ with entries in $\{1, 2, 3, \ldots, r\}$. We first associate a tableau $\mathfrak{T} \in \mathcal{B}_\lambda$ with any Gelfand-Tsetlin pattern. The top row of the pattern is the shape λ of $\mathfrak{T}$. Removing the cells labeled r from the tableau results in the shape that is the second row of the Gelfand-Tsetlin pattern, etc. This procedure is reversible and so there is another bijection between $\mathcal{B}_\lambda$ and Gelfand-Tsetlin patterns with top row λ. We may compose this with our previous bijection between $\mathfrak{S}_{\mathbf{z},\lambda}$ and Gelfand-Tsetlin patterns. Given an admissible state $\mathfrak{s}$, we will denote the associated tableau by $\mathfrak{T}(\mathfrak{s})$.

For example with the state $\mathfrak{s}$ in Fig. 1, we have

$$\text{GTP}(\mathfrak{s}) = \left\{ \begin{matrix} 4 & & 2 & & 0 \\ & 2 & & 1 & \\ & & 1 & & \end{matrix} \right\}, \quad \text{GTP}^\circ(\mathfrak{s}) = \left\{ \begin{matrix} 2 & & 1 & & 0 \\ & 1 & & 1 & \\ & & 1 & & \end{matrix} \right\}, \quad \mathfrak{T}(\mathfrak{s}) = \begin{array}{|c|c|} \hline 1 & 3 \\ \hline 2 \\ \cline{1-1} \end{array}.$$

The set $\mathcal{B}_\lambda$ has the structure of a Kashiwara-Nakashima crystal of tableaux (see [34,18]). As such it comes with a weight map $\text{wt} : \mathcal{B}_\lambda \longrightarrow \Lambda$, where $\Lambda \simeq \mathbb{Z}^r$ denotes the weight lattice for $G = \text{GL}(r)$. If $\mathfrak{T} \in \mathcal{B}_\lambda$, then identifying Λ with $\mathbb{Z}^r$, we define $\text{wt}(\mathfrak{T}) = (\mu_1, \cdots, \mu_r)$ where μ_i is the number of entries in $\mathfrak{T}$ equal to i.

Proposition 3.2. *Let $\lambda \in \Lambda$ be a dominant weight and $\mathfrak{s} \in \mathfrak{S}_{\mathbf{z},\lambda}$ be an admissible state of the uncolored five-vertex model defined above.*

(i) *The Boltzmann weight $\beta(\mathfrak{s})$ and the weight map of the associated tableau $\mathfrak{T}(\mathfrak{s})$ are related by*

$$\beta(\mathfrak{s}) = \mathbf{z}^{\rho + w_0 \, \text{wt}(\mathfrak{T}(\mathfrak{s}))}.$$

(ii) *The partition function of an ensemble $\mathfrak{S}_{\mathbf{z},\lambda}$ is related to Schur functions by*

$$Z(\mathfrak{S}_{\mathbf{z},\lambda}) = \mathbf{z}^\rho \, s_\lambda(\mathbf{z}).$$

To illustrate (i), in the example of Fig. 1, we have

$$\beta(\mathfrak{s}) = z_1^3 z_2^2 z_3, \quad \mathbf{z}^\rho = z_1^2 z_2, \quad \text{and} \quad \mathbf{z}^{w_0 \, \text{wt}(\mathfrak{T}(\mathfrak{s}))} = z_1 z_2 z_3.$$

Proof of Proposition 3.2. To prove (i), note that from the weights in Fig. 2 a vertex in the i-th row contributes a factor of z_i if and only if the spin to the left of the vertex is $-$. Hence the power of z_i equals the number of $-$ spins on the horizontal edges in the i-th row, not counting the $-$ on the right boundary edge. Now such $-$ occur on the horizontal edges between the $A_{i,j}$ and $A_{i+1,j+1}$ columns, or to the right of the $A_{i,r}$ column. Hence the power of z_i in $\mathfrak{S}_{\mathbf{z},\lambda}$ is

$$\sum_{j=i}^{r} A_{i,j} - \sum_{j=i}^{r-1} A_{i+1,j+1} = \left(\sum_{j=i}^{r} a_{i,j} - \sum_{j=i+1}^{r} a_{i+1,j} \right) + r - i.$$

The term in parentheses is the number of $r + 1 - i$ entries in the tableau $\mathfrak{T}(\mathfrak{s})$. Taking the product over all i gives (i).

Using (i) and the combinatorial formula

$$s_\lambda(\mathbf{z}) = \sum_{\mathfrak{T}} \mathbf{z}^{\mathrm{wt}\,\mathfrak{T}}$$

for the Schur function we have $Z(\mathfrak{S}_{\mathbf{z},\lambda}) = \mathbf{z}^\rho \, s_\lambda(w_0 \mathbf{z})$. Part (ii) now follows from the symmetry of the Schur function. □

Alternatively, we can evaluate the partition function using a local symmetry known as the Yang-Baxter equation, which is Theorem 3.3 below. To state this we need to introduce a new type of vertices that we will call rotated vertices. These vertices are rotated by 45 degrees counterclockwise and there are two parameters z_i, z_j associated to each vertex. We denote such rotated vertices by R_{z_i,z_j} (here we use R as their Boltzmann weights may be alternately viewed as entries of an R-matrix that "solves" a lattice model). These vertices can be attached to the grid systems we defined before, like the one in Fig. 1 to obtain new systems. It is by working with these new systems that we can use the Yang-Baxter equation and derive functional equations for the partition function of our initial system (the one without any rotated vertices).

The Boltzmann weights of the rotated vertices are different from the Boltzmann weights of the regular vertices and are given in Fig. 3.
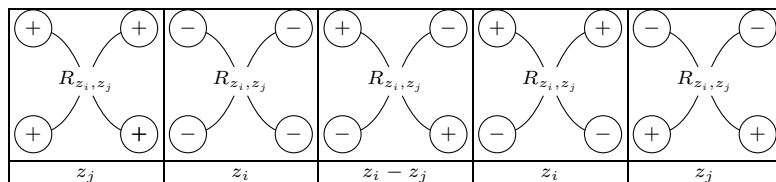
Fig. 3. The R-matrix for the uncolored system. From [10] we know that we may regard this combinatorial R-matrix as the "crystal limit" of the $U_q(\widehat{\mathfrak{gl}}(1|1))$ R-matrix when $q \to 0$.

Now consider the following two miniature systems that contain both regular and rotated vertices:

$$(3.2)$$
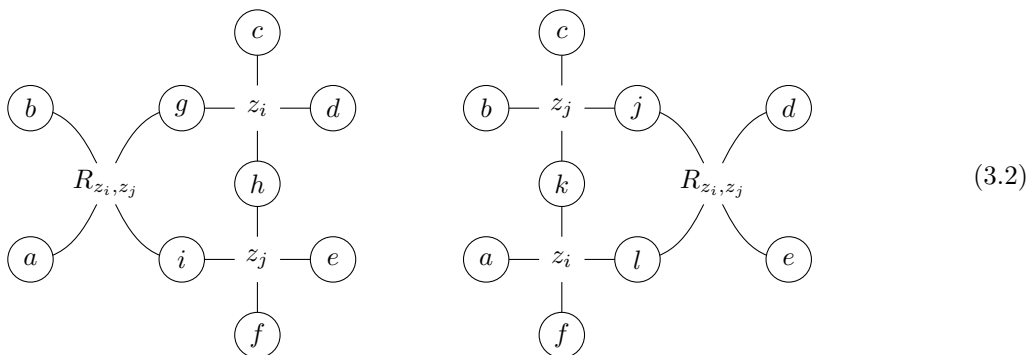
Here, as with the system defined before, we fix the spins of the exterior edges (a, b, c, d, e, f). An assignment of spins to the interior edges is again called a state. Both systems have a partition function defined by summing the weights of the admissible states made from all possible assignments of spins to the interior edges (g, h, i in the left system, or j, k, l on the right). The weight of the entire state is computed just as above: we take a product of the weights of each vertex using the weights of the regular vertices that are given in Fig. 2 and the weights of the rotated vertices that are given in Fig. 3.

For example if $(a, b, c, d, e, f) = (+, -, +, -, +, +)$ there is only one choice $(g, h, i) = (-, +, +)$ that gives a nonzero contribution to the first system, and the partition function is the Boltzmann weight $z_i z_j$ of this state. For the second system, there are two states with nonzero contribution, namely $(j, k, l) = (-, +, +)$, with weight z_j^2 and $(+, -, -)$ with weight $z_j(z_i - z_j)$. The partition function again equals $z_i z_j$.

Theorem 3.3. *Let $a, b, c, d, e, f \in \{+, -\}$. Then the partition functions of the two systems in* (3.2) *are equal.*

Proof. This is a special case of a Yang-Baxter equation found in [12]. Referring to the arXiv version of the paper, the Boltzmann weights are in Table 1 of that paper with $t_i = 0$.   □

The symmetry of the Schur function may be easily deduced from this via a procedure called the "train argument" that amounts to repeated use of Theorem 3.3 on a larger grid system with an attached rotated vertex as later illustrated in Fig. 8 for the colored five-vertex model. See also [12, Lemma 4], leading to an alternate proof of the evaluation of the partition function.

The models of this section may be described as the "uncolored" (or equivalently "one-colored") version of our five-vertex models. They were known before the writing of this paper. In the next section, we present a generalization known as colored models, which are new. We will prove a Yang-Baxter equation in the colored setting (Theorem 4.2) that

will then be used to relate the partition function of the lattice models to the Demazure atoms.

4. Colored ice models for $GL(r)$

There are multiple ways to depict admissible states of the six-vertex model. Many of these are described in Chapter 8 of Baxter's inspiring book [4]. In particular, rather than using spins or arrows to decorate edges, one can instead use the presence or absence of a line (or "path") along an edge. These are the "line configurations" in [4], Figure 8.2. Our convention will be that the presence of a line corresponds to a $-$ spin, so that admissible states may be viewed as a collection of paths moving downward and rightward through the lattice. Inspired by ideas of Borodin and Wheeler [9] in the context of certain other solvable lattice models, we may assign colors to each such path to refine the partition function of the prior section to produce polynomial Demazure atoms.

First we describe the relevant solvable colored lattice model. Just as before, upon fixing a dominant weight $\lambda = (\lambda_1, \ldots, \lambda_r)$, we begin with a rectangular lattice of $N + 1$ columns ($N \geqslant \lambda_1 + r - 1$) and r rows whose edges are to be assigned spins $\pm$ according to a five-vertex model. Moreover, to each edge with $-$ spin, we assign a "color," an additional attribute from a finite set $\{c_1, \cdots, c_r\}$ of size equal to the number of rows in the model. We will order these colors by $c_1 > c_2 > \cdots > c_r$. By a *colored spin* we mean either $+$, or a color c_i. For the purpose of comparing with the uncolored system, we regard a colored spin c_i as a spin $-$ with an extra piece of data, namely a color.

To each dominant weight λ, we now define $r!$ distinct partition functions. Given $w \in W = S_r$ and a vector of colors $\mathbf{c} = (c_1, \cdots, c_r)$, let $w\mathbf{c}$ be the permuted vector of colors, that is $(w\mathbf{c})_i = c_{w^{-1}i}$. We will call such vectors of colors *flags*. Now assign boundary conditions to the colored lattice model as follows. To the vertical top boundary edges, we assign spins $-$ in the columns labeled $\lambda_i + r - i$ as before ($1 \leqslant i \leqslant r$). Now however we also need to assign colors to these edges, and we assign the color c_i to the $\lambda_i + r - i$ column. Each edge along the right boundary is also assigned a $-$ spin, but here we assign the colors $w\mathbf{c}$ in order from top to bottom. Just as before, all remaining boundary spins along the bottom, left, and top are $+$.

Admissible states are then assignments of colored spins to the interior edges such that every vertex has adjacent spins as in Fig. 4 with the understanding that the colors red > blue may be replaced by any colors c_i and c_j with $c_i > c_j$. Boltzmann weights for each vertex are listed in the figure as well. We denote the resulting system of admissible states as $\mathfrak{S}_{\mathbf{z}, \lambda, w}$. The configurations in Fig. 4 ensure that each color will determine a path, moving downward and rightward through the lattice. The choice of $w \in W$ then specifies the row where each colored path exits the right-hand boundary. As before, we denote by $Z(\mathfrak{S}_{\mathbf{z}, \lambda, w})$ the partition function of the colored lattice model.

For example, let $r = 3$. We will denote the three colors c_1, c_2 and c_3 as R (red), B (blue) and G (green) in the figures. Take $w = s_1 s_2$. Then $\mathbf{c} = (R, B, G)$ and $w\mathbf{c} = (G, R, B)$. With $\lambda = (2, 1, 0)$ the system $\mathfrak{S}_{\mathbf{z}, \lambda, w}$ has two states, which are illustrated in Fig. 5.

Fig. 4. Colored Boltzmann weights for two colors c_i and c_j, portrayed as red (R) and blue (B). We assume that red > blue. If the configuration is not in the table, the weight is zero. The weights are not quite symmetric in the colors, since in the $\mathbf{a_2}$ patterns, the smaller of the two involved colors (blue) is not allowed on the right edge and the larger color is not allowed on the bottom edge. With our boundary conditions, the patterns with four edges all red or blue could be omitted, but this would change the R-matrix in Fig. 6; see Remark 4.3. This would not affect the results of this paper, but we prefer these weights for consistency with the uncolored case. (For colored versions of this and subsequent figures, the reader is referred to the web version of this article.)

Proposition 4.1. *For any dominant weight λ, $\mathfrak{S}_{\mathbf{z},\lambda} = \bigsqcup_{w \in W} \mathfrak{S}_{\mathbf{z},\lambda,w}$ (disjoint union) where a colored spin c_i is mapped to spin $-$, and hence*

$$Z(\mathfrak{S}_{\mathbf{z},\lambda}) = \sum_{w \in W} Z(\mathfrak{S}_{\mathbf{z},\lambda,w}).$$

Proof. We may begin with a state of the uncolored system and assign colors to the edges with $-$ spins. Along the top row, assign color c_i to the $-$ spin in column $\lambda_i + r - i$ as directed for colored ice states. We will argue that there is a unique way of coloring the remaining $-$ spins that is consistent with the configurations in Fig. 4.

The boundary spins on the left edge are all $+$, so they do not need colors assigned. After this, we proceed inductively, rightwards and downwards row by row, adding color to the $-$ spins of the state using the weights from Fig. 4. The key observation is that at a vertex labeled as follows:
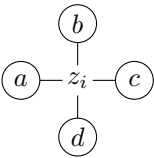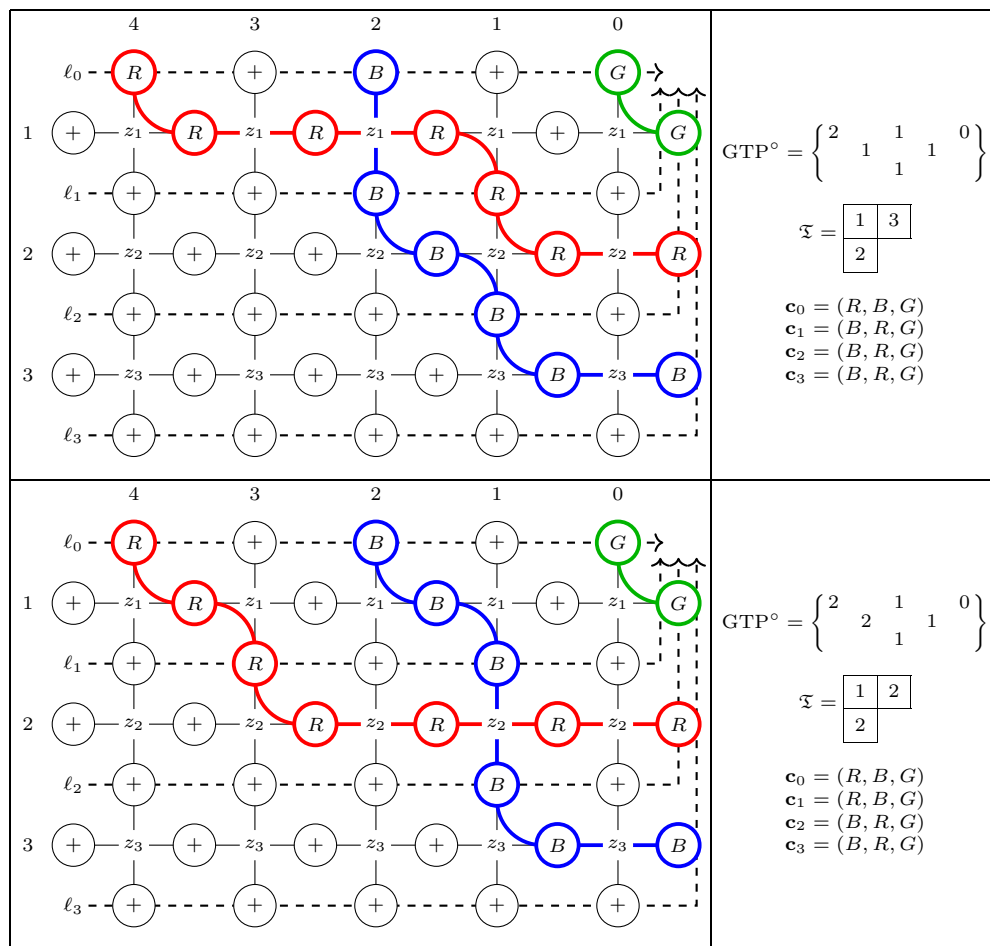
Fig. 5. The two states of the system $\mathfrak{S}_{\mathbf{z},(2,1,0),s_1s_2}$ where $\mathbf{c} = (R, B, G)$ (red, blue, green) and $w\mathbf{c} = s_1s_2\mathbf{c} = (G, R, B)$. The dashed lines ℓ_i, and the intermediate flags $\mathbf{c}_i$ will be used in the proof of Theorem 6.1. Each intermediate flag $\mathbf{c}_i$ is the sequence of colors through the line ℓ_i, and is obtained from the previous $\mathbf{c}_{i-1}$ by interchanging some colors on the vertical edges that intersect it. Because ℓ_{r-1} only intersects one vertical edge, no interchanges are possible at the last step, meaning that $\mathbf{c}_{r-1} = \mathbf{c}_r$. Note that, while the flag $w\mathbf{c} = s_1s_2\mathbf{c} = (G, R, B)$ denoting the right boundary condition is read from the top down, the last line ℓ_3 intersects the same edges from the bottom up. Thus, $\mathbf{c}_3 = w_0s_1s_2\mathbf{c} = (B, R, G)$.

the colored spins a and b and the spins $\pm$ of c and d determine a unique color at c and d with non-zero weight according to Fig. 4. Indeed, colored spin is conserved at a vertex, meaning that the total incoming (top and left) colored spins counted with multiplicity equals the total outgoing (bottom and right) colored spins. Moreover for the a_2 configurations if a and b are of different colors, then d will be the smaller of the two colors. We see that the assignment of colors is completely deterministic, and the colored state falls into a unique one of the ensembles $\mathfrak{S}_{\mathbf{z},\lambda,w}$.
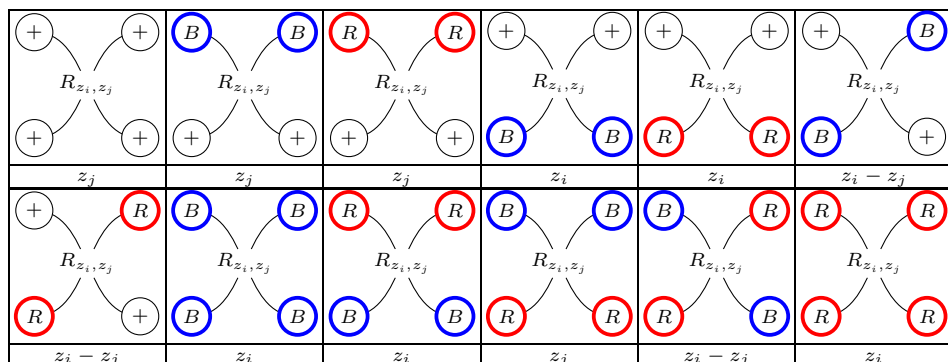
Fig. 6. The colored R-matrix.

Now mapping colored spins c_i to spin $-$, the colored Boltzmann weights of Fig. 4 map to the uncolored Boltzmann weights of Figs. 2, thus proving both statements. □
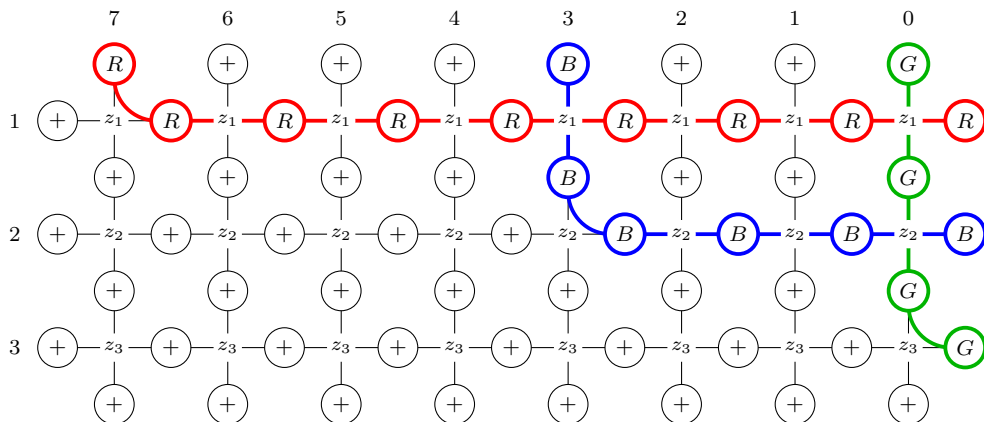
There is again a Yang-Baxter equation.

Theorem 4.2. *Using the Boltzmann weights in Fig. 4 for the regular vertices and the R-matrix in Fig. 6 for the rotated vertices, let a, b, c, d, e, f be colored spins. Then the partition functions of the (now colored) systems depicted in* (3.2) *are equal.*

Proof. In order for either side of (3.2) to be nonzero, each color that appears on a boundary edge a, b, c, d, e, f must appear an even number of times (and therefore at least twice), since otherwise according to Figs. 4 and 6, the Boltzmann weight of the state is zero. Therefore at most 3 colors can appear among a, b, c, d, e, f and the interior edges cannot involve any further colors. Thus there are only a fixed finite number ($4^6 = 4096$) of cases to be considered (independent of the number of colors r), and this can easily be checked using a computer. (To check this we used the Sage mathematical software.) □

Remark 4.3. It may be checked that the colored R-matrix (with r colors) in Fig. 6 is the limit as $q \to \infty$ of the R-matrix of a Drinfeld twist of $U_q\big(\widehat{\mathfrak{sl}}(r|1)\big)$. It is also possible to vary the Boltzmann weights as follows: in Fig. 4, omit the $\mathbf{a_2}$ patterns in which all four edges have the same color; and in Fig. 6, change the Boltzmann weights of the patterns in which all four edges have the same color from z_i to z_j. These changes do not affect any of the arguments in this paper since the changed patterns do not appear in any of the states of the systems we consider, but they change the underlying quantum group to a Drinfeld twist of $U_q\big(\widehat{\mathfrak{sl}}_{r+1}\big)$.

Our next result shows that the colored partition function with r colors and r rows is a polynomial Demazure atom for $\mathrm{GL}(r)$ up to a factor of $\mathbf{z}^\rho$.

$$\mathrm{GTP}(\mathfrak{s}) = \left\{ \begin{matrix} 7 & & 3 & & 0 \\ & 3 & & 0 & \\ & & 0 & & \end{matrix} \right\}, \quad \mathrm{GTP}^\circ(\mathfrak{s}) = \left\{ \begin{matrix} 5 & & 2 & & 0 \\ & 2 & & 0 & \\ & & 0 & & \end{matrix} \right\},$$

$$\mathfrak{T}(\mathfrak{s}) = \begin{array}{|c|c|c|c|c|} \hline 2 & 2 & 3 & 3 & 3 \\ \hline 3 & 3 \\ \cline{1-2} \end{array}, \quad \mathrm{string}_{(1,2,1)}(\mathfrak{T}) = \begin{bmatrix} \textcircled{0} & \textcircled{0} \\ & \textcircled{0} \end{bmatrix}.$$

Fig. 7. The ground state. In this unique state with maximal number of crossings of colored lines, we have $\beta(\mathfrak{s}) = \mathbf{z}^{\lambda+\rho}$, $\mathrm{wt}(\mathfrak{T}(\mathfrak{s})) = \mathbf{z}^{w_0(\lambda+\rho)}$. Note that since we read the "flag" of colors on the right edge from top to bottom, it is this ground state corresponding to $w = 1$ that has the maximum number of crossings.

Theorem 4.4. *For every $w \in W$ we have*

$$Z(\mathfrak{S}_{\mathbf{z},\lambda,w}) = \mathbf{z}^\rho \partial_w^\circ \mathbf{z}^\lambda.$$

Proof. The proof is by induction with respect to Bruhat order. If $w = 1_W$, it is easy to see that there is a unique state in $\mathfrak{S}_{\mathbf{z},\lambda,1_W}$ and its Boltzmann weight is $\mathbf{z}^{\rho+\lambda}$ (see Fig. 7). Thus it suffices to show that for each s_i and w with $s_i w > w$,

$$\mathbf{z}^{-\rho} Z(\mathfrak{S}_{\mathbf{z},\lambda,s_i w}) = \partial_i^\circ \left(\mathbf{z}^{-\rho} Z(\mathfrak{S}_{\mathbf{z},\lambda,w}) \right). \tag{4.1}$$

Let $w\mathbf{c} = \mathbf{d} = (d_1, \cdots, d_r)$. Since $s_i w > w$, we have $d_i > d_{i+1}$. Consider the partition function of the system in Fig. 8 (top). This is a system like the one portrayed in Fig. 5 but with an attached rotated vertex z_{i+1}, z_i on the left. We only exhibit two of the rows of the system because this is where the interesting changes occur. Also note that the parameters of the two rows are flipped, so now the top row has parameter z_{i+1} and the bottom row has parameter z_i.

Consulting Fig. 6, the rotated vertex (or the R-matrix) has only one possible admissible configuration (with all + spins). This means the partition function of the top system in Fig. 8 will be equal to the Boltzmann weight of
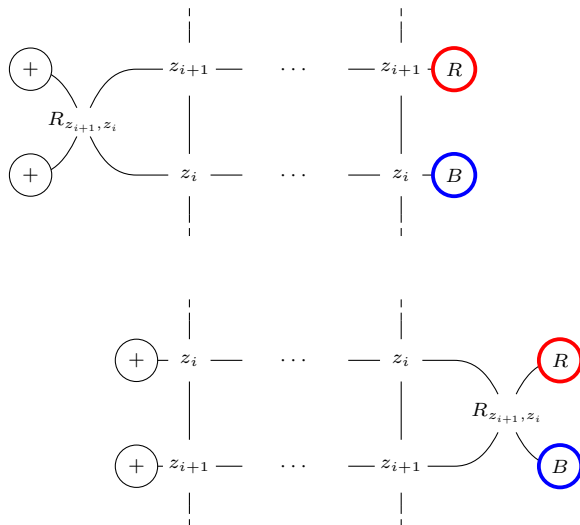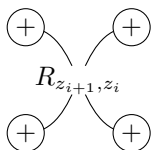
Fig. 8. Top: the system $\mathfrak{S}_{s_i \mathbf{z}, \lambda, w}$ with the R-matrix attached. Bottom: after using the Yang-Baxter equation.

times the partition function of the system with the rotated vertex removed. This is then $z_i Z(\mathfrak{S}_{s_i \mathbf{z}, \lambda, w})$. Note that z_i and z_j in Fig. 6 become here z_{i+1} and z_i, respectively. We are using red and blue for the colors d_i and d_{i+1}, respectively.

After repeated use of the Yang-Baxter equation (Fig. (3.2)), we move the rotated vertex to the right, switch the parameters of the two rows and obtain a system with the same partition function by Theorem 4.2. This is the system on the bottom of Fig. 8. This method of Baxter is sometimes called the "train argument."

Now looking at the possible weights from Fig. 6, the R-matrix has two admissible configurations (third and fifth on the second row) and so the equality of partition functions from Fig. 8 becomes the identity

$$z_i Z(\mathfrak{S}_{s_i \mathbf{z}, \lambda, w}) = z_{i+1} Z(\mathfrak{S}_{\mathbf{z}, \lambda, w}) + (z_{i+1} - z_i) \, Z(\mathfrak{S}_{\mathbf{z}, \lambda, s_i w}).$$

Since $\mathbf{z}^{\alpha_i} = z_i / z_{i+1}$, the above identity may be rewritten as

$$Z(\mathfrak{S}_{\mathbf{z}, \lambda, s_i w}) = -(1 - \mathbf{z}^{\alpha_i})^{-1} (Z(\mathfrak{S}_{\mathbf{z}, \lambda, w}) - \mathbf{z}^{\alpha_i} Z(\mathfrak{S}_{s_i \mathbf{z}, \lambda, w})). \tag{4.2}$$

The right-hand side can be interpreted as the operator $-(1 - \mathbf{z}^{\alpha_i})^{-1}(1 - \mathbf{z}^{\alpha_i} s_i)$ applied to $Z(\mathfrak{S}_{\mathbf{z}, \lambda, w})$. Note that

$$\partial_i^\circ = -(1 - \mathbf{z}^{\alpha_i})^{-1}(1 - s_i), \quad \text{and hence} \quad \mathbf{z}^\rho \partial_i^\circ \mathbf{z}^{-\rho} = -(1 - \mathbf{z}^{\alpha_i})^{-1}(1 - \mathbf{z}^{\alpha_i} s_i).$$

Using this, (4.1) follows from (4.2). $\square$

Remark 4.5. It was recently found by Brubaker, Bump and Friedberg that a variation of the Boltzmann weights produces the Demazure character $\mathbf{z}^\rho \partial_w \mathbf{z}^\lambda$ instead of the Demazure atom $\mathbf{z}^\rho \partial_w^\circ \mathbf{z}^\lambda$ in Theorem 4.4. The modification is to interchange red and blue in the third case of Fig. 4. This will be discussed in a subsequent paper.

5. Demazure crystals and atoms

A refined Demazure character formula in the context of crystals was obtained by Littelmann [44] and Kashiwara [32] for any symmetrizable Kac-Moody Cartan type. We begin this section by reviewing this refinement for finite Cartan types. Then, after introducing string data on a crystal, we specialize to Cartan Type A and describe an important map σ from the crystal to the Weyl group which allows us to identify Demazure atoms with subsets of the highest weight crystal and characterize the vertices belonging to this crystal. This result (Theorem 5.5) is one of the main results in this paper and its proof is ultimately completed in Section 8.

Let us fix a finite Cartan type with weight lattice Λ. Let λ be a dominant weight, which we assume to be a partition. Then there is a unique irreducible representation π_λ of highest weight λ, and a corresponding normal crystal $\mathcal{B}_\lambda$ whose character is the same as that of π_λ.

Recall that crystals come equipped with Kashiwara maps $e_i, f_i : \mathcal{B}_\lambda \to \mathcal{B}_\lambda \cup \{0\}$ and $\varphi_i, \varepsilon_i : \mathcal{B}_\lambda \to \mathbb{Z}$ (see [34]). For a crystal $\mathcal{B}$ an element v is called a *highest weight element* if $e_i(v) = 0$ for all i; similarly it is *lowest weight* if all $f_i(v) = 0$. The crystal $\mathcal{B}_\lambda$ has unique highest and lowest weight elements v_λ and $v_{w_0\lambda}$, respectively; with weights $\mathrm{wt}(v_\lambda) = \lambda$ and $\mathrm{wt}(v_{w_0\lambda}) = w_0\lambda$.

With $\mathcal{B} = \mathcal{B}_\lambda$ let $\mathbb{Z}[\mathcal{B}]$ be the free abelian group on $\mathcal{B}$. We define a map $\partial_i : \mathcal{B} \longrightarrow \mathbb{Z}[\mathcal{B}]$ in terms of the Kashiwara operators e_i and f_i by

$$\partial_i v = \begin{cases} v + f_i v + \ldots + f_i^k v & \text{if } k \geqslant 0, \\ 0 & \text{if } k = -1, \\ -(e_i v + \ldots + e_i^{-k-1} v) & \text{if } k < -1, \end{cases}$$

where $k = \langle \mathrm{wt}(v), \alpha_i^\vee \rangle$. This lifts the Demazure operator ∂_i to the crystal; indeed, composing with the familiar weight map on the crystal (described in Section 3) produces the Demazure operators of (2.1), and so we will use the same notation for the operator in both contexts.

By an *i-root string* we mean an equivalence class of elements of $\mathcal{B}$ under the equivalence relation that $x \equiv y$ if $x = e_i^r y$ or $x = f_i^r y$ for some r. An i-root string S has a unique

highest weight element u_S characterized by $e_i(u_S) = 0$. We may now state the *refined Demazure character formula* of Littelmann and Kashiwara.

Theorem 5.1 *(Littelmann, Kashiwara). Let $\mathcal{B} = \mathcal{B}_\lambda$.*

(i) *There exist subsets $\mathcal{B}(w)$ of $\mathcal{B}$ indexed by $w \in W$ such that $\mathcal{B}(1) = \{v_\lambda\}$, $\mathcal{B}(w_0) = \mathcal{B}$ and if $s_i w > w$ then*

$$\mathcal{B}(s_i w) = \{x \in \mathcal{B} \mid e_i^r x \in \mathcal{B}(w) \text{ for some } r\} \ .$$

(ii) *If S is an i-root string then $\mathcal{B}(w) \cap S$ is one of the three possibilities: $\varnothing$, S or $\{u_S\}$.*

(iii) *We have*

$$\sum_{x \in \mathcal{B}(w)} \mathbf{z}^{\mathrm{wt}(x)} = \partial_w \mathbf{z}^\lambda \ .$$

See [32] or [18] Chapter 13 for proof.

Demazure characters and atoms were defined in Section 2 as functions on the complex torus T. The preceding theorem allows us to lift Demazure characters to the crystal $\mathcal{B} = \mathcal{B}_\lambda$; as in the theorem, we will denote these (lifted) Demazure characters by $\mathcal{B}(w)$ for $w \in W$. Let $\mathcal{B}^\circ(w)$ ($w \in W$) be a family of disjoint subsets of $\mathcal{B}$. We call these a family of *crystal Demazure atoms* if

$$\mathcal{B}(w) = \bigcup_{y \leqslant w} \mathcal{B}^\circ(y). \tag{5.1}$$

Lemma 5.2. *If a family of disjoint subsets $\mathcal{B}^\circ(w)$ satisfying (5.1) exists it is unique.*

Proof. Let us identify a subset S of $\mathcal{B}$ with the element $\sum_{v \in S} v$ of the free abelian group $\mathbb{Z}[\mathcal{B}]$. Then we may rewrite (5.1) as

$$\mathcal{B}(w) = \sum_{y \leqslant w} \mathcal{B}^\circ(y).$$

By Möbius inversion with respect to the Bruhat order ([54,52]) this is equivalent to

$$\mathcal{B}^\circ(w) = \sum_{y \leqslant w} (-1)^{\ell(w) - \ell(y)} \mathcal{B}(y).$$

This characterization of $\mathcal{B}^\circ(w)$ as an element of $\mathbb{Z}[\mathcal{B}]$ proves the uniqueness. $\square$

For the remainder of the section, we specialize to Cartan Type A. As explained in the Introduction, in a decomposition of the set of tableaux in a $\mathrm{GL}(r)$ crystal $\mathcal{B}_\lambda$ is given by the theory of Lascoux-Schützenberger keys. We will give another algorithm to compute,

for any $v \in \mathcal{B}$, the element $w \in W$ such that $v \in \mathcal{B}^\circ(w)$ and show that the resulting subsets satisfy (5.1), making them a family of crystal Demazure atoms. This algorithm makes use of the *string* or *BZL* patterns for vertices in a crystal, which we now describe. These patterns were introduced in [5] for Type A, and more generally in [45]. See also [18] Chapter 11 and [13] Chapters 2 and 5.

Let $\mathbf{i} = (i_1, \cdots, i_N)$ be a reduced word for $w_0 = s_{i_1} \cdots s_{i_N}$. Given any $v \in \mathcal{B}_\lambda$, let $b_1 := b_1(v)$ be the largest nonnegative integer such that $f_{i_1}^{b_1} v \neq 0$. Then let b_2 be the largest integer such that $f_{i_2}^{b_2} f_{i_1}^{b_1} v \neq 0$. Continuing, we obtain $f_{i_N}^{b_N} \cdots f_{i_2}^{b_2} f_{i_1}^{b_1} v = v_{w_0\lambda}$ as explained in [45]. We will denote the resulting vector of lengths in root strings by

$$\text{string}_{\mathbf{i}}^{(f)}(v) := (b_1, \cdots, b_N). \tag{5.2}$$

Dually, let $c_1, \cdots, c_N$ be the maximum values such that $e_{i_k}^{c_k} \cdots e_{i_2}^{c_2} e_{i_1}^{c_1} v \neq 0$ for $k = 1, 2, \cdots, N$. Then $e_{i_N}^{c_N} \cdots e_{i_2}^{c_2} e_{i_1}^{c_1} v = v_\lambda$ and we define

$$\text{string}_{\mathbf{i}}^{(e)}(v) := (c_1, \cdots, c_N). \tag{5.3}$$

The map $\alpha \mapsto -w_0\alpha$ permutes the positive roots, and in particular the simple roots. Thus there is a bijection $i \mapsto i'$ of the set I of indices such that $\alpha_{i'} = -w_0\alpha_i$ and $w_0 s_i w_0^{-1} = s_{i'}$. In the $\mathrm{GL}(r)$ case $I = \{1, \cdots, r-1\}$ and $i' = r - i$. The crystal also has a map $v \mapsto v'$, the *Schützenberger* or *Lusztig* involution, such that if $v \in \mathcal{B}$ then

$$f_i(v') = (e_{i'}(v))', \qquad e_i(v') = (f_{i'}(v))'. \tag{5.4}$$

It follows from (5.4) that if $\mathbf{i}' = (i_1', \cdots, i_N')$ then

$$\text{string}_{\mathbf{i}'}^{(e)}(v) = \text{string}_{\mathbf{i}}^{(f)}(v'). \tag{5.5}$$

Littelmann [45] observed that for certain "good" choices of long word $\mathbf{i}$ the set of possible string patterns can be easily characterized. Although Littelmann gives good word choices for the classical Cartan types, our results are mainly for Type A and we will specialize to the $\mathrm{GL}(r)$ case for the remainder of this section, indeed for the rest of the paper. For $\mathrm{GL}(r)$, one such Littelmann good word is

$$\mathbf{i} = (1, 2, 1, 3, 2, 1, 4, 3, 2, 1, \cdots, r, r-1, \cdots, 3, 2, 1). \tag{5.6}$$

Thus

$$\mathbf{i}' = (r-1, r-2, r-1, r-3, r-2, r-1, \cdots, r-3, r-2, r-1). \tag{5.7}$$

Following [45] we arrange the string pattern $\text{string}_{\mathbf{i}'}^{(e)}(v) = (b_1, b_2, \cdots)$ in an array

$$
\text{string}_{\mathbf{i}'}^{(e)}(v) = \begin{bmatrix} \ddots & & \vdots & \vdots \\ & b_4 & b_5 & b_6 \\ & & b_2 & b_3 \\ & & & b_1 \end{bmatrix} \tag{5.8}
$$

in which the b_i satisfy the Littelmann cone inequalities

$$
b_1 \geqslant 0, \qquad b_2 \geqslant b_3 \geqslant 0, \qquad b_4 \geqslant b_5 \geqslant b_6 \geqslant 0, \qquad \cdots. \tag{5.9}
$$

Following [13] we decorate the string pattern (5.8) by circling certain b_i according to these cone inequalities.

Circling Rule 5.3. *Let* $\mathbf{b} = (b_1, b_2, \cdots, b_N)$ *where* $N = r(r-1)/2$ *be a sequence of nonnegative integers satisfying* (5.9). *We arrange the sequence in an array* (5.8) *and decorate it by circling an entry* b_i *if it is minimal in the cone. Explicitly, if i is a triangular number, so that* b_i *is at the right end of its row, the condition for circling it is that* $b_i = 0$; *otherwise, the condition for circling is that* $b_i = b_{i+1}$.

Let $(i_1, i_2, i_3, i_4, i_5, i_6, \cdots)$ be the sequence $(1, 2, 1, 3, 2, 1, \cdots)$ of (5.6). We transfer the circles from the string pattern to the following array made with the simple reflections:

$$
\begin{bmatrix} \ddots & & \vdots & \vdots \\ & s_{i_6} & s_{i_5} & s_{i_4} \\ & & s_{i_3} & s_{i_2} \\ & & & s_{i_1} \end{bmatrix} = \begin{bmatrix} \ddots & & \vdots & \vdots \\ & s_1 & s_2 & s_3 \\ & & s_1 & s_2 \\ & & & s_1 \end{bmatrix}. \tag{5.10}
$$

Remark 5.4. Note that the horizontal orders of the entries in (5.8) and (5.10) are different.

If $v \in \mathcal{B}_\lambda$, let $(s_{j_1}, \cdots, s_{j_k})$ be the subsequence of $(s_{i_1}, s_{i_2}, s_{i_3}, \cdots) = (s_1, s_2, s_1, s_3, s_2, s_1, \cdots)$ consisting of the circled reflections in (5.10) derived from the string pattern $\text{string}_{\mathbf{i}'}^{(e)}(v)$. Here $\mathbf{i}'$ is the specific sequence in (5.7). With the nondescending product Π_{nd} defined in (1.2), define $\sigma : \mathcal{B}_\lambda \to W$ by

$$
\sigma(v) := \Pi_{\text{nd}}(s_{j_1}, \cdots, s_{j_k}). \tag{5.11}
$$

For example, suppose that the string pattern is:

$$
\begin{bmatrix} \textcircled{1} & 1 \\ & \textcircled{0} \end{bmatrix}. \tag{5.12}
$$

The circling rule tells us to circle b_1 and b_2 since $b_1 = 0$ and $b_2 = b_3$. Thus we circle these entries:

$$\begin{bmatrix} \boxed{s_1} & s_2 \\ & \boxed{s_1} \end{bmatrix}$$

and $\sigma(v) = \Pi_{\mathrm{nd}}(s_1, s_1) = \left\{ S_1^2 \right\} = s_1$ in this case, using the notation of Remark 1.1.

We may now state one of our main results. Let W_λ be the stabilizer of λ in W. Note that if $w, w' \in W$ lie in the same coset of W/W_λ then $\mathcal{B}_\lambda(w) = \mathcal{B}_\lambda(w')$. We will say that $w \in W$ is λ-maximal if it is the longest element of its coset.

Theorem 5.5. *Let $\mathcal{B} = \mathcal{B}_\lambda$ be the $\mathrm{GL}(r)$ crystal of tableaux with highest weight λ. There exist a family of subsets $\mathcal{B}^\circ(w)$ of $\mathcal{B}$ indexed by $w \in W$ such that $\mathcal{B}^\circ(w) = \mathcal{B}^\circ(w')$ if and only if w, w' lie in the same coset of W/W_λ; otherwise they are disjoint, and such that the decomposition (5.1) is satisfied. If w is the longest element of this coset, then*

$$\mathcal{B}^\circ(w) = \{v \in \mathcal{B} \mid w_0\sigma(v) = w\}. \tag{5.13}$$

If w is not the longest element of its coset then the equation $w_0\sigma(v) = w$ has no solutions.

This is a refinement of results of Lascoux and Schützenberger [42], and is one of the main points of the paper. Equation (5.13), together with the definition and properties of σ, leads to the algorithmic characterization of the crystal Demazure atom in Subsection 1.1. The proof of Theorem 5.5 will be given later, in Section 8. One may check that the definition of σ in (5.11) agrees with the one derived from reduced pipe dreams in Section 1.4 of [36] (and originally in [24]) under a natural bijection between such pipe dreams and states of our lattice models.

6. A bijection between colored states and Demazure atoms

We return now to colored ice models and their relation to crystals for $\mathrm{GL}(r)$. Recall from Proposition 4.1 that the admissible states of colored ice $\mathfrak{S}_{\mathbf{z},\lambda,w}$ with $w \in W$ partition the set of admissible states of uncolored ice in the system $\mathfrak{S}_{\mathbf{z},\lambda}$. The map from any $\mathfrak{S}_{\mathbf{z},\lambda,w}$ to $\mathfrak{S}_{\mathbf{z},\lambda}$ is simply given by ignoring the colors (i.e., replacing each colored edge by a $-$ spin). In Section 3 we defined a map $\mathfrak{s} \to \mathfrak{T}(\mathfrak{s})$ from $\mathfrak{S}_{\mathbf{z},\lambda}$ to $\mathcal{B}_\lambda$. In this section, we characterize the image of $\mathfrak{S}_{\mathbf{z},\lambda,w}$ under this map. This will be a key ingredient in the proof of Theorem 5.5 in Section 8.

Let $v \to v'$ be the Schützenberger (Lusztig) involution of $\mathcal{B}_\lambda$.

Theorem 6.1. *If $w \in W$ and $\mathfrak{s} \in \mathfrak{S}_{\mathbf{z},\lambda}$, then $\mathfrak{s} \in \mathfrak{S}_{\mathbf{z},\lambda,w}$ if and only if $w_0\sigma\big(\mathfrak{T}(\mathfrak{s})'\big) = w$.*

Thus once Theorem 5.5 is proved, we may compare Theorem 6.1 with (5.13) to see that the map $\mathfrak{s} \to \mathfrak{T}(\mathfrak{s})'$ sends the ensemble $\mathfrak{S}_{\mathbf{z},\lambda,w}$ to the Demazure atom $\mathcal{B}_\lambda^\circ(w)$.

Before we prove Theorem 6.1 we give an example. In Fig. 9, we have labeled the elements of the $\mathrm{GL}(3)$ crystal $\mathcal{B}_\lambda$ ($\lambda = (2, 1, 0)$) by a flag indicating the colors along the

right edge of the corresponding state. These colors are read off from top to bottom on the horizontal edges at the right boundary of the grid. In the decomposition of Proposition 4.1, the flag is a permutation $w\mathbf{c}$ of the colors of the standard flag, which we are taking to be $\mathbf{c} = (R, B, G)$. For example, to compute the flags for the elements

$$
\boxed{\begin{array}{cc} 1 & 3 \\ 2 & \end{array}} \quad \text{and} \quad \boxed{\begin{array}{cc} 1 & 2 \\ 2 & \end{array}} \tag{6.1}
$$

we construct the corresponding states as in Fig. 5 and then read off the colors from the right edge, which are (G, R, B) for both states. In Fig. 9 these colors are represented as a flag. The flag allows us to read off the unique $y \in W$ such that the corresponding state $\mathfrak{s}$ is in $\mathfrak{S}_{\mathbf{z}, \lambda, y}$. For example in the two states in (6.1), we have the flag $(G, R, B) = s_1 s_2 (R, B, G)$ and so $y = s_1 s_2$.

Now let us also verify Theorem 5.5 and Theorem 6.1 for the patterns in Fig. 5. Both are in the system $\mathfrak{S}_{\mathbf{z},(2,1,0),s_1 s_2}$. Their string patterns $\mathrm{string}_{\mathbf{i}'}^{(e)}(\mathfrak{T}') = \mathrm{string}_{\mathbf{i}}^{(f)}(\mathfrak{T})$ are shown in Table 1.
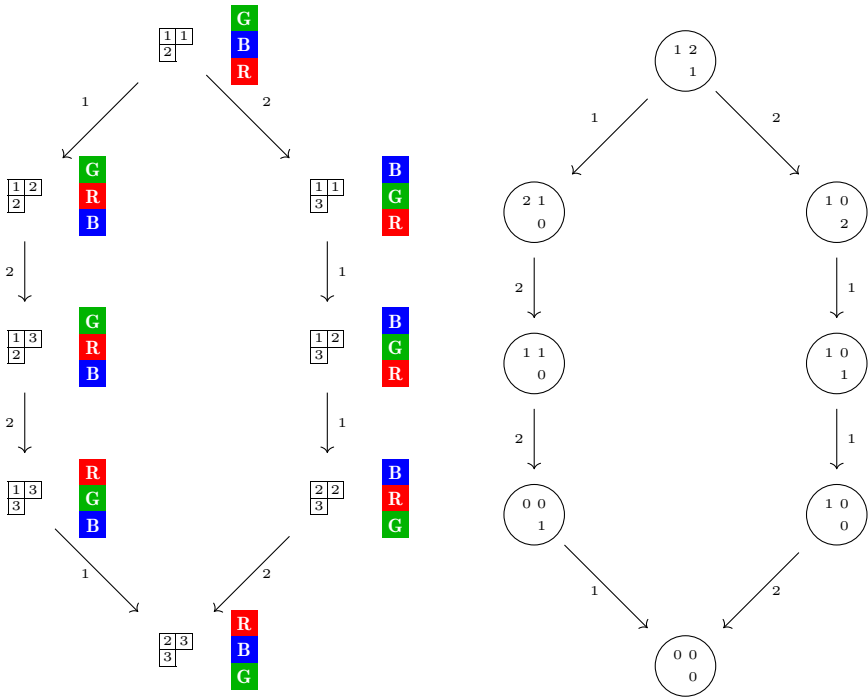
Fig. 9. Left: The GL(3) crystal of highest weight $\lambda = (2, 1, 0)$, showing the "flags" that are the colors of the right edges of the corresponding states, read from top to bottom. The highest weight element is at the top. Right: the same crystal, showing the pattern $\mathrm{string}_{\mathbf{i}}^{(f)}$ that controls both the crossings of colored lines in the state, and which also carry information about the Demazure crystals.

Table 1
String patterns for the examples shown in Fig. 5 with tableau $\mathfrak{T}$ and its Schützenberger involution $\mathfrak{T}'$.

$\mathfrak{T}$	$\mathfrak{T}'$	$\mathrm{string}_{(1,2,1)}^{(f)}(\mathfrak{T}) = \mathrm{string}_{(2,1,2)}^{(e)}(\mathfrak{T}')$
$\begin{array}{cc} 1 & 2 \\ 2 & \end{array}$	$\begin{array}{cc} 2 & 2 \\ 3 & \end{array}$	$\begin{bmatrix} 2 & 1 \\ & \textcircled{0} \end{bmatrix}$
$\begin{array}{cc} 1 & 3 \\ 2 & \end{array}$	$\begin{array}{cc} 1 & 2 \\ 3 & \end{array}$	$\begin{bmatrix} \textcircled{1} & 1 \\ & \textcircled{0} \end{bmatrix}$

We have $\sigma(\mathfrak{T}') = s_1$ in both cases; indeed for the first row in Table 1, $\sigma(\mathfrak{T}') = \Pi_{\mathrm{nd}}(s_1) = s_1$ and in the second row $\sigma(\mathfrak{T}') = \Pi_{\mathrm{nd}}(s_1, s_1) = s_1$, and in both cases $w_0\sigma(\mathfrak{T}') = s_1 s_2$. Moreover the two patterns $\mathfrak{T}'$ comprise the Demazure atom $\mathcal{B}^\circ(s_1 s_2)$ since they are the two patterns in $\mathcal{B}(s_1 s_2)$ that are not already in $\mathcal{B}(s_2)$. Thus we have confirmed both Theorem 5.5 and Theorem 6.1 for one particular Demazure atom.

Proof of Theorem 6.1. First we will show that the circled locations in $\mathrm{GTP}^\circ(\mathfrak{s})$ correspond to $\mathtt{a}_2$ vertices in the state $\mathfrak{s}$ (by the labeling in Fig. 4), which are places where the colored lines may cross.

Let $\mathfrak{s}$ be a state of $\mathfrak{S}_{\mathbf{z},\lambda,y}$. Let $\mathrm{GTP}^\circ(\mathfrak{s})$ and $\mathfrak{T} \in \mathcal{B}_\lambda$ be the corresponding Gelfand-Tsetlin pattern and tableau as described in Section 3 (using the embedding of $\mathfrak{S}_{\mathbf{z},\lambda,y}$ into $\mathfrak{S}_{\mathbf{z},\lambda}$). We take $v = \mathfrak{T}'$ in (5.8) so we are using $\mathrm{string}_{\mathbf{i}'}^{(e)}(\mathfrak{T}') = \mathrm{string}_{\mathbf{i}}^{(f)}(\mathfrak{T})$ represented as a vector $(b_1, b_2, \cdots)$. Let us consider how the circles may be read off from the Gelfand-Tsetlin pattern with entries $a_{i,j}$ as in (3.1). According to Proposition 2.2 of [13],

$$
\begin{aligned}
b_1 &= a_{r,r} - a_{r-1,r} \\
b_2 &= (a_{r-1,r-1} + a_{r-1,r}) - (a_{r-2,r-1} + a_{r-2,r}), \\
b_3 &= a_{r-1,r} - a_{r-2,r}, \\
b_4 &= (a_{r-2,r-2} + a_{r-2,r-1} + a_{r-2,r}) - (a_{r-3,r-2} + a_{r-3,r-1} + a_{r-3,r}), \\
b_5 &= (a_{r-2,r-1} + a_{r-2,r}) - (a_{r-3,r-1} + a_{r-3,r}), \\
b_6 &= a_{r-2,r} - a_{r-3,r}, \\
&\vdots
\end{aligned}
\tag{6.2}
$$

These imply that the circled locations depend on equalities between entries in $\mathrm{GTP}(\mathfrak{s})$ or, equivalently, $\mathrm{GTP}^\circ(\mathfrak{s})$. For example b_2 is circled if and only if $a_{r-1,r-1} = a_{r-2,r-1}$. With $A_{i,j}$ the entries in $\mathrm{GTP}(\mathfrak{s})$, so that $A_{i,j} = a_{i,j} + r - j$, this is equivalent to $A_{r-1,r-1} = A_{r-2,r-1}$, and similarly if any b_k is circled then we have $A_{i,j} = A_{i-1,j}$ for the appropriate

i, j. Now recall that in the bijection $\mathfrak{T} \leftrightarrow \mathfrak{s}$, $A_{i,j}$ is the number of a column where a vertical edge has a colored spin. Therefore from the admissible colored ice configurations of Fig. 4, the circled entries in (5.8) correspond to vertices of type $\mathtt{a_2}$ in the state of ice $\mathfrak{s}$. These are locations where two colored lines may cross. From Fig. 4 the lines will cross if and only if the left edge color is greater than the top edge color at the vertex, which is equivalent to the assumption that they have not crossed previously.

We consider a sequence of lines ℓ_i through the grid, $i = 0, \ldots, r$ to be described as follows. The line ℓ_i begins to the left of the grid between the i-th and $(i+1)$-th row, or above the first row if $i = 0$, or below the r-th row if $i = r$. It traverses the grid, then moves up to the northeast corner. See Fig. 5 where these lines are drawn in two examples.

Each ℓ_i intersects exactly r colored lines, and we can read off the colors sequentially; let $\mathbf{c}^i$ be the corresponding sequence of colors. Thus $\mathbf{c}^0 = \mathbf{c}$, while $\mathbf{c}^r = w_0 y \mathbf{c}$, where y is the Weyl group element we wish to compute. The w_0 in this last identity is included because the line ℓ_r visits the horizontal edges on the right edge from bottom to top, whereas in describing the flag $y\mathbf{c}$, the reading is from top to bottom. (See Fig. 5.)

As we have already noted, the circled entries in (5.8) correspond to $\mathtt{a_2}$ patterns in the state. These are places where two colored lines may cross. The crossings interchange colors and each corresponds to a simple reflection that is circled in (5.10). So if $i > 0$ we may try to compute $\mathbf{c}_i$ from $\mathbf{c}_{i-1}$ by applying the circled reflections in the i-th row of (5.10). Remembering from the proof of Proposition 4.1 that the colors in the i-th row are assigned from right to left, this means (subject to a caveat that we will explain below) that

$$\mathbf{c}_i = (s_{r-i})_i \cdots (s_3)_i (s_2)_i (s_1)_i \mathbf{c}_{i-1},$$

where $(s_j)_i$ denotes s_j if s_j is circled in the i-th row of (5.10), and $(s_j)_i = 1$ if s_j is not circled.

If $i = r$, there is no i-th row to (5.10), and correspondingly $\mathbf{c}_r = \mathbf{c}_{r-1}$. This is as it should be since at this stage there is only a single colored vertical edge that intersects the line ℓ_{r-1}, and no interchanges are possible. (See Fig. 5.)

We mentioned that there is a caveat in the above explanation. This is because from Fig. 4 we see that in an $\mathtt{a_2}$ vertex, if the color c is left of the vertex and d is above, the colored lines will cross if $c > d$ but not otherwise. In particular, two colored lines can only cross once. More precisely, if two colored lines meet more than once (at $\mathtt{a_2}$ vertices) they will cross the first time they meet, and never again. For this reason, the permutation that turns $\mathbf{c}^0 = \mathbf{c}$ into $\mathbf{c}^r = w_0 y \mathbf{c}$ is the nondescending product $\Pi_{\mathrm{nd}}(s_{i_1}, \cdots, s_{i_k})$ where $(s_{i_1}, \cdots, s_{i_k})$ is the subsequence of circled simple reflections in (5.10). Note that according to the definition of $\Pi_{\mathrm{nd}}(s_{i_1}, \cdots, s_{i_k})$ in equation (1.2), the circled simple reflections corresponding to the $\mathtt{a_2}$ patterns where there is a crossing play a role in recursively defining $\Pi_{\mathrm{nd}}(s_{i_1}, \cdots, s_{i_k})$, while the circled simple reflections

corresponding to the $\mathtt{a}_2$ patterns where there is no crossing do not affect the product. Therefore $y = w_0 \, \Pi_{\mathrm{nd}}(s_{i_1}, \cdots, s_{i_k}) = w_0\sigma(\mathfrak{T}')$.

This shows that $\mathfrak{s} \in \mathfrak{S}_{\mathbf{z},\lambda,y}$ implies $y = w_0\sigma(\mathfrak{T}(\mathfrak{s})')$. By Proposition 4.1, if $\mathfrak{s} \notin \mathfrak{S}_{\mathbf{z},\lambda,y}$ then $\mathfrak{s} \in \mathfrak{S}_{\mathbf{z},\lambda,y'}$ with $y \neq y' \in W$, which we have shown implies that $y \neq y' = w_0\sigma(\mathfrak{T}')$. $\square$

Proposition 6.2. *Suppose that a part of λ is repeated, so that $\lambda_i = \lambda_{i+1} = \ldots = \lambda_j = c$. Then each pair of colored lines through the top boundary edges in columns $c+r-i, \cdots, c+r-j$ must cross. Thus if $\mathfrak{S}_{\mathbf{z},\lambda,w}$ is nonempty, then w is the shortest Weyl group element in its coset in W/W_λ.*

Proof. We are only considering states in which there are no $\mathtt{b}_1$ patterns since these have weight 0 in Fig. 4. We leave it to the reader to convince themselves that because of this, colored lines that start in adjacent columns, or more generally in columns not separated by a + spin on the top boundary edge must cross. Because we read the colors on the top boundary vertical edges from left to right and on the right horizontal boundary edges from top to bottom, this means that the colors are in the same order. Hence if $\mathfrak{S}_{\mathbf{z},\lambda,w}$ is nonempty, w does not change the order of colors corresponding to equal parts in the partition λ. This is the same as saying that it is the shortest element of its coset in W/W_λ. $\square$

Corollary 6.3. *If $v \in \mathcal{B}_\lambda$ then $\sigma(v)$ is the longest element of its coset in W/W_λ.*

Proof. Let $\mathfrak{s}$ be the state such that $\mathfrak{T}(\mathfrak{s})' = v$. Then $\mathfrak{s} \in \mathfrak{S}_{\mathbf{z},\lambda,w}$ with $w = w_0\sigma(v)$ by Proposition 4.1 and Theorem 6.1. Thus, according to Proposition 6.2, $w_0\sigma(v)$ is the shortest element in its coset and therefore $\sigma(v)$ is the longest element of its coset. $\square$

7. Demazure atoms in $\mathcal{B}_\infty$

The results in this and the subsequent sections are for Cartan type A. Before we can prove Theorem 5.5 in the next section, we will need to introduce two tools: a lift to an infinite crystal $\mathcal{B}_\infty$ and an involution on this crystal. Both will be defined later in this section and they will be used to show the inclusion $\mathcal{B}_\lambda(w) \subseteq \{v \in \mathcal{B}_\lambda \mid w_0\sigma(v) \leqslant w\}$, by first showing its $\mathcal{B}_\infty$-analogue in Lemma 7.6. In Section 8 we will then show that this is actually an equality, proving Theorem 5.5, using input from the lattice model results in the previous sections. A summary of how we will prove these statements is illustrated in Fig. 10 and will be detailed further below.

Although Littelmann [44] proved the refined Demazure character formula Theorem 5.1 for many semisimple Lie algebras using tableaux methods, Kashiwara [32] introduced the two tools mentioned above to prove it completely for symmetrizable Kac-Moody Lie algebras.

The first innovation in [32] is to prove the formula indirectly by working not with $\mathcal{B}_\lambda$ but with the infinite crystal $\mathcal{B}_\infty$ that is the crystal base of a Verma module. That is,
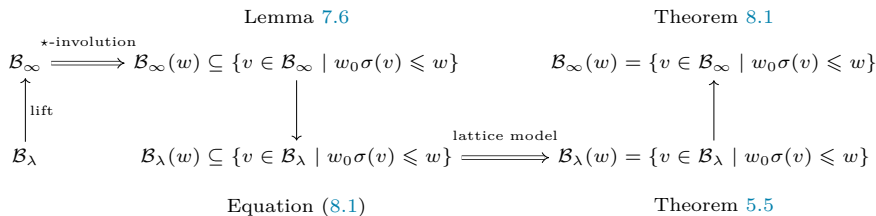
Fig. 10. Summary of arguments used in Sections 7 and 8 to prove Theorem 5.5, one of the main results of this paper, and its analog for $\mathcal{B}_\infty$ Theorem 8.1.

Theorem 5.1 is true for $\mathcal{B}_\infty$ as well as $\mathcal{B}_\lambda$ meaning that we also have Demazure crystals $\mathcal{B}_\infty(w)$ for $\mathcal{B}_\infty$. One may embed $\mathcal{B}_\lambda$ into $\mathcal{B}_\infty$, and the preimage of the Demazure crystal $\mathcal{B}_\infty(w)$ in $\mathcal{B}_\infty$ is the Demazure crystal $\mathcal{B}_\lambda(w)$. In [32,18,31] proofs of the refined Demazure character formula proceed by proving a version on $\mathcal{B}_\infty$ first.

The second innovation in [32] is to make use of an involution $\star$ which, as we will explain, interchanges two natural parametrizations of the crystal by elements of a convex cone in $\mathbb{Z}^N$.

In proving Theorem 5.5 we will use both of these ideas from [32], namely to lift the problem to $\mathcal{B}_\infty$ crystal and to exploit the properties of the $\star$-involution. Two references adopting a point of view similar to Kashiwara's are Bump and Schilling [18] and Joseph [31]. Both these references treat the Demazure character formula in the context of $\mathcal{B}_\infty$ and the $\star$-involution.

The notion of crystal Demazure atoms can be adapted to $\mathcal{B}_\infty$; we define these to be subsets $\mathcal{B}^\circ(w)$ that are disjoint and satisfy (5.1). By Lemma 5.2 these conditions determine the atoms.

For Type A the existence of a family of crystal Demazure atoms for $\mathcal{B}_\infty$ will be proved in Corollary 8.2 in the next section. In fact, the characterizations of $\mathcal{B}(w)$ and $\mathcal{B}^\circ(w)$ for Type A in terms of the function σ translate readily to $\mathcal{B}_\infty$. The $\star$-involution of $\mathcal{B}_\infty$ is not a crystal graph automorphism, but it has other important properties. In particular, it maps the Demazure crystal $\mathcal{B}(w)$ into $\mathcal{B}(w^{-1})$. So using the $\star$-involution we are able to reformulate Theorem 5.5, or more precisely the corresponding identity for $\mathcal{B}_\infty(w)$, as the identity

$$\mathcal{B}_\infty(w^{-1}) = \{v \in \mathcal{B} \mid w_0\sigma(v^\star) \leqslant w\}. \tag{7.1}$$

The definition of σ for $\mathcal{B}_\lambda$ was given in terms of Gelfand-Tsetlin patterns, but it may be restated in terms of string data (5.8). As we will explain later in this section, the $\star$-involution transforms the string data into other natural data. (See (7.3).) In Lemma 7.4 below we have an explicit formula for $\sigma(v^\star)$ in terms of this data. Thus (7.1) becomes amenable to proof. The main details are in the proof of Lemma 7.5, which contains partial information about how $\sigma(v^\star)$ changes when f_k is applied to v. The proof of this lemma is technical, but the starting point is the formula (7.11) for $f_k(v)$ in terms of

data that we have in hand due to Lemma 7.3. Once Lemma 7.5 is proved, we conclude this section with Lemma 7.6 which makes progress towards showing (7.1) by proving the inclusion of the left-hand side in the right-hand side.

Then, using the information that we have obtained from the Yang-Baxter equation in Theorem 4.4, we can leverage this inclusion to prove Theorem 5.5 in Section 8. Note that this is a statement about $\mathcal{B}_\lambda$, not $\mathcal{B}_\infty$. Equation (7.1) is equivalent to Theorem 8.1, which is proved after Theorem 5.5 by going back to $\mathcal{B}_\infty$. Theorem 8.1 would of course imply Theorem 5.5, but we prove Theorem 5.5 first where we can apply Theorem 4.4. Thus we go back and forth between $\mathcal{B}_\infty$ and $\mathcal{B}_\lambda$ in order to prove everything. Finally in Corollary 8.2 we obtain a characterization of crystal Demazure atoms in $\mathcal{B}_\infty$.

In [32,18], the construction of $\mathcal{B}_\infty$ for any Cartan type depends on the choice of a reduced decomposition of the long Weyl group element $w_0 = s_{i_1} \cdots s_{i_N}$. A main feature of the theory is that the crystal is independent of this choice of decomposition; to change to another reduced decomposition one may apply piecewise linear maps to all data. On the other hand, Littelmann [45] showed that one particular choice of reduced word is especially nice, and it is this Littelmann word that is important for us. Given this choice, elements of the crystal are parametrized by data from which we can read off the Demazure atoms.

We recall Kashiwara's definition of $\mathcal{B}_\infty$ for an arbitrary Cartan type before specializing to the $\mathrm{GL}(r)$ (Cartan Type A_{r-1}) crystal. (For further details and proofs see [32] and Chapter 12 of [18].)

If $i \in I$, the index set for the simple reflections, let $\mathcal{B}_i$ be the elementary crystal defined in [32] Example 1.2.6 or [18] Section 12.1. This crystal has one element $u_i(a)$ of weight $a\alpha_i$ for every $a \in \mathbb{Z}$ on which the crystal operators e_i and f_i act as $e_i(u_i(a)) = u_i(a+1)$ and $f_i(u_i(a)) = u_i(a-1)$. Let $\mathbf{i} = (i_1, \cdots, i_N)$ be a sequence of indices such that $w_0 = s_{i_N} \cdots s_{i_1}$ is a reduced expression of the long Weyl group element and let

$$\mathcal{B}_{\mathbf{i}} = \mathcal{B}_{i_1} \otimes \cdots \otimes \mathcal{B}_{i_N} \ .$$

Remark 7.1. We recall that there is a difference between notation for tensor product of crystals between [32] and [18]. We will follow the second reference, so to read Kashiwara or Joseph, reverse the order of tensor products, interpreting $x \otimes y$ as $y \otimes x$.

Let $u_0 = u_{i_1}(0) \otimes \cdots \otimes u_{i_N}(0) \in \mathcal{B}_{\mathbf{i}}$, and let $\mathfrak{C}_{\mathbf{i}}$ be the subset of $\mathbb{Z}^N$ consisting of all elements $\mathbf{a} = (a_1, \cdots, a_N)$ such that

$$u_{\mathbf{i}}(\mathbf{a}) = u(\mathbf{a}) = u_{i_1}(-a_1) \otimes \cdots \otimes u_{i_N}(-a_N) \tag{7.2}$$

can be obtained from u_0 by applying some succession of crystal operators f_i. Then $\mathfrak{C}_{\mathbf{i}}$ is the set of integer points in a convex polyhedral cone in $\mathbb{R}^N$. We regard $\mathfrak{C}_{\mathbf{i}}$, embedded via the map $\mathbf{a} \mapsto u(\mathbf{a})$ to be a subcrystal of $\mathcal{B}_{\mathbf{i}}$; this requires redefining $e_i(v) = 0$ if $\varepsilon_i(v) = 0$. With this exception, the Kashiwara operators e_i, f_i, ε_i and φ_i are the same

as for the ambient crystal $\mathcal{B}_\mathbf{i}$. If $\mathbf{j}$ is another reduced expression for w_0 then there is a piecewise-linear bijection $\mathfrak{C}_\mathbf{i} \longrightarrow \mathfrak{C}_\mathbf{j}$ that is an isomorphism of crystals; in this sense the crystal $\mathfrak{C}_\mathbf{i}$ is independent of the choice of word $\mathbf{i}$. The crystal $\mathcal{B}_\infty$ is defined to be this crystal.

In $\mathcal{B}_\infty$ the element u_0 is the unique highest weight element, and the unique element of weight 0. If $x \in \mathcal{B}_\infty$ then, as with the finite crystals $\mathcal{B}_\lambda$, the integer $\varepsilon_i(x)$ is nonnegative and equals the number of times e_i may be applied to x, i.e. $\varepsilon_i(x) = \max\{k | e_i^k(x) \neq 0\}$. On the other hand $f_i(x)$ is never 0, so $\varphi_i(x)$ has no such interpretation. It still has meaning and the identity $\varphi_i(x) - \varepsilon_i(x) = \langle \mathrm{wt}(x), \alpha_i^\vee \rangle$ holds.

Because $f_i(x)$ is never 0, the string patterns $\mathrm{string}_\mathbf{i}^{(f)}(v)$ cannot be defined for $\mathcal{B}_\infty$ since the sequence $f_i^k v$ never terminates. However $\mathrm{string}_\mathbf{i}^{(e)}(v)$ can be defined by (5.3). Interestingly, for each reduced word $\mathbf{i}$ representing w_0, the set $\{\mathrm{string}_\mathbf{i}^{(e)}(v) \mid v \in \mathcal{B}_\infty\}$ coincides with the cone $\mathfrak{C}_\mathbf{i}$. However the data $\mathbf{a}$ such that (7.2) holds is *not* the string data. Rather, there is a weight-preserving bijection $\star : \mathcal{B}_\infty \to \mathcal{B}_\infty$ of order two such that

$$\mathbf{a} = \mathrm{string}_\mathbf{i}^{(e)}(v^\star), \qquad v = u_\mathbf{i}(\mathbf{a}) . \tag{7.3}$$

This is true for any reduced word $\mathbf{i}$, and $\star$ is independent of $\mathbf{i}$. This is Kashiwara's $\star$-*involution*. See [32], [18] and [31]. Equation (7.3) is Theorem 14.16 in [18], or see the proof of Proposition 3.2.3 in [31].

Let λ be a dominant weight. There is a crystal $\mathcal{T}_\lambda$ with a single element t_λ of weight λ; then $\mathcal{T}_\lambda \otimes \mathcal{B}_\infty$ is a crystal identical to $\mathcal{B}_\infty$ except that the weights of its elements are all shifted by λ. Thus its highest weight element is $t_\lambda \otimes u_0$ with weight λ. If $\mathcal{B}_\lambda$ is the crystal with highest weight λ, then $\mathcal{B}_\lambda$ may be embedded in $\mathcal{T}_\lambda \otimes \mathcal{B}_\infty$ by mapping the highest weight vector v_λ to $t_\lambda \otimes u_0$. Let $\psi_\lambda : \mathcal{B}_\lambda \to \mathcal{B}_\infty$ be the map such that $v \mapsto t_\lambda \otimes \psi_\lambda(v)$ is this embedding of crystals.

Demazure crystals are defined for $\mathcal{B} = \mathcal{B}_\infty$ as follows. If $w = 1$ then $\mathcal{B}(w) = \{u_0\}$. Then recursively: if s_i is a simple reflection such that $s_i w > w$ we define $\mathcal{B}(s_i w)$ to be the set of all $v \in \mathcal{B}$ such that $e_i^k v \in \mathcal{B}(w)$ for some $k \geqslant 0$. Theorem 5.1 (i) remains valid for $\mathcal{B}_\infty$. The theory of Demazure crystals for $\mathcal{B}_\infty$ is related to the theory for $\mathcal{B}_\lambda$ by the fact that $\mathcal{B}_\lambda(w)$ is the preimage of the corresponding $\mathcal{B}_\infty$ Demazure crystal under the embedding of $\mathcal{B}_\lambda$ into $\mathcal{T}_\lambda \otimes \mathcal{B}_\infty$. See [32] and [18] Chapters 12 and 13.

Now we specialize to $\mathrm{GL}(r)$ crystals; the Cartan type is A_{r-1}. If we use either the Littelmann word (5.6) or $\mathbf{i}'$ in (5.7) then the cone $\mathfrak{C}_\mathbf{i}$ is characterized by the inequalities (5.9). See [45] Theorem 5.1 or [13], Proposition 2.2. Now ψ_λ is a crystal morphism, so if $v \in \mathcal{B}_\lambda$ then

$$\mathrm{string}_{\mathbf{i}'}^{(e)}(\psi_\lambda(v)) = \mathrm{string}_{\mathbf{i}'}^{(e)}(v).$$

Thus we may define $\sigma : \mathcal{B}_\infty \to W$ by (5.11) and if $v \in \mathcal{B}_\lambda$ then $\sigma(\psi_\lambda(v)) = \sigma(v)$. Then we may define $\mathcal{B}^\circ(w)$ by (5.13) also for $\mathcal{B} = \mathcal{B}_\infty$ and $\mathcal{B}_\infty^\circ(w)$ is the preimage of $\mathcal{B}_\lambda^\circ(w)$ under the map ψ_λ.

Let $\mathbf{i}$ be as in (5.7) so that $\mathbf{i}' = (1, 2, 1, 3, 2, 1, \cdots)$. Let

$$v = D_1 \otimes \cdots \otimes D_{r-1} \in \mathcal{B}_\infty \subset \mathcal{B}_{\mathbf{i}}, \qquad D_i \in \mathcal{B}_{r-i} \otimes \cdots \otimes \mathcal{B}_{r-1}. \tag{7.4}$$

Specifically we may write

$$D_i = D_i(v) = u_{r-i}(-d_{i,r-i}) \otimes \cdots \otimes u_{r-1}(-d_{i,r-1}) = \bigotimes_{j=r-i}^{r-1} u_j(-d_{i,j}). \tag{7.5}$$

Remembering (7.3), for v to be in $\mathcal{B}_\infty$ the entries $d_{ij} = d_{ij}(v)$ must lie in the Littelmann cone (5.9), which in our present notation is determined by the inequalities

$$d_{i,j} \geqslant d_{i,j+1}, \qquad (r - i \leqslant j \leqslant i).$$

Let $c_{i,j} = c_{i,j}(v) = d_{i,j} - d_{i,j+1} \geqslant 0$.

Remark 7.2. Initially $d_{i,j}$ is defined if $r - i \leqslant j \leqslant r - 1$ but we extend this to $j = r$ with the convention that $d_{i,r} = 0$. Hence by this convention $c_{i,r-1} = d_{i,r-1}$. This convention will prevent certain cases having to be treated separately.

By [18] Lemma 2.33 the function φ_k (part of the data defining a crystal) is given by

$$\varphi_k(v) = \max_i(\Phi_{i,k}(v)) \tag{7.6}$$

where

$$\Phi_{i,k} = \Phi_{i,k}(v) = \varphi_k(D_i) + \sum_{\ell < i} \langle \mathrm{wt}(D_\ell), \alpha_k^\vee \rangle .$$

Lemma 7.3. *Assume that* $r - k \leqslant i \leqslant r - 1$. *Then*

$$\varphi_k(D_i) = \begin{cases} c_{i,k-1} & \text{if } k > r - i; \\ -d_{i,k} & \text{if } k = r - i, \end{cases} \tag{7.7}$$

and

$$\Phi_{i,k} - \Phi_{i+1,k} = c_{i,k} - c_{i+1,k-1}. \tag{7.8}$$

Proof. First assume that $r - k + 1 \leqslant i \leqslant r - 1$. Then using Lemma 2.33 of [18] again, $\varphi_k(D_i)$ is the maximum over $r - i \leqslant j \leqslant r - 1$ of

$$\varphi_k(u_j(-d_{i,j})) + \left\langle \sum_{r-i \leqslant \ell < j} -d_{i,\ell}\alpha_\ell, \, \alpha_k^\vee \right\rangle.$$

By the definition of the elementary crystal ([18] Section 12.1) we have $\varphi_k(u_j(-d_{i,j})) = -\infty$ unless $j = k$, so

$$\varphi_k(D_i) = \varphi_k(u_k(-d_{i,k})) + \left\langle \sum_{r-i \leqslant \ell < k} -d_{i,\ell}\alpha_\ell, \, \alpha_k^\vee \right\rangle = -d_{i,k} + d_{i,k-1} = c_{i,k-1}$$

proving (7.7). Here we have used the fact that $\varphi_k(u_k(-a)) = -a$, as well as $\langle \alpha_\ell, \alpha_k^\vee \rangle = -1$ if $l = k \pm 1$ and 2 if $l = k$, and 0 otherwise. Now

$$\Phi_{i,k} - \Phi_{i+1,k} = \varphi_k(D_i) - \varphi_k(D_{i+1}) - \langle \mathrm{wt}(D_i), \alpha_k^\vee \rangle$$

and with $r - k + 1 \leqslant i \leqslant r - 1$ we have (using Remark 7.2 if $k = r - 1$)

$$\langle \mathrm{wt}(D_i), \alpha_k^\vee \rangle = d_{i,k-1} - 2d_{i,k} + d_{i,k+1} = c_{i,k-1} - c_{i,k}.$$

Combining this with (7.7) we obtain (7.8). The case $k = r - i$ is similar, except that $d_{i,k-1}$ is replaced by zero where it appears. $\square$

We now wish to use some nondescending products. We will use the notation of Remark 1.1. Let

$$\Omega_i(D_i) = \prod_{\substack{1 \leqslant j \leqslant i \\ c_{i,r-1+j-i}=0}} S_j \, . \tag{7.9}$$

Define $\sigma^\dagger : \mathcal{B}_\infty \to W$ by

$$\sigma^\dagger(v) = \{\Omega_{r-1}(D_{r-1}) \cdots \Omega_1(D_1)\} \, . \tag{7.10}$$

From Remark 1.1 the brackets $\{\cdot\}$ here mean that the product is taken in the degenerate Hecke algebra, then the resulting basis vector is replaced by the corresponding Weyl group element.

Lemma 7.4. *We have*

$$\sigma^\dagger(v) = \sigma(v^\star)^{-1}.$$

Proof. By (7.3), the string pattern $\mathrm{string}_{\mathbf{i}'}^{(e)}(v^\star)$ is the sequence $(b_1, b_2, \ldots)$ such that

$$v = u_{i_1'}(-b_1) \otimes u_{i_2'}(-b_2) \otimes \cdots \, .$$

Put these into an array as in (5.8) and circle entries as in Circling Rule 5.3. Thus the b_k are the $d_{i,j}$ in the order determined by (7.4) and (7.5). Since $c_{i,j} = d_{i,j} - d_{i,j+1}$ (with the caveat in Remark 7.2) we see that if b_k equals $d_{i,j}$, it is circled if and only if $c_{i,j} = 0$. Recall that

$$\sigma(v^\star) = \Pi_{\mathrm{nd}}(s_{j_1}, \cdots, s_{j_k}) = \{S_{j_1} \cdots S_{j_k}\}$$

where $s_{j_1}, s_{j_2}, \cdots$ are the circled elements. Now $S_{j_1}, S_{j_2}, \cdots$ are exactly the entries that appear in the product (7.10), but they appear in reverse order; so what we get is $\sigma(v^\star)^{-1}$. $\square$

Lemma 7.5. *We have either* $\sigma^\dagger(v) = \sigma^\dagger(f_k v)$ *or* $\sigma^\dagger(v) = s_k \sigma^\dagger(f_k v)$.

Proof. Let p be the first value of i where $\Phi_{i,k}(v)$ attains its maximum. By [18] Lemma 2.33

$$f_k(v) = D_1 \otimes \cdots \otimes f_k(D_p) \otimes \cdots \otimes D_{r-1}. \tag{7.11}$$

Furthermore, by applying the same Lemma to $f_k(D_p)$ and using the fact that $\varphi_k(u_j(-d_{i,j})) = -\infty$ unless $j = k$ we have

$$f_k(D_p) = u_{r-p}(-d_{p,r-i}) \otimes \cdots \otimes u_k(-d_{p,k} - 1) \otimes \cdots \otimes u_{r-1}(-d_{p,r-1})$$

meaning that f_k acting on v has the effect that $d_{p,k}$ is replaced by $d_{p,k} + 1$.

We factor $\Omega_p(D_p) = \Omega'_p(D_p)\Omega''_p(D_p)$ where

$$\Omega'_p(D_p) = \prod_{\substack{1 \leqslant j \leqslant k+p-r \\ c_{p,r-1+j-p}=0}} S_j, \qquad \Omega''_p(D_p) = \prod_{\substack{k+p-r+1 \leqslant j \leqslant p \\ c_{p,r-1+j-p}=0}} S_j \ .$$

We will prove that

$$\Omega'_p(D_p)\Omega''_p(D_p) = \Omega''_p(D_p)\Omega'_p(D_p), \qquad \Omega'_p(f_k D_p)\Omega''_p(f_k D_p) = \Omega''_p(f_k D_p)\Omega'_p(f_k D_p). \tag{7.12}$$

Indeed, every S_j above with $1 \leqslant j \leqslant k+p-r$ commutes with every $S_{j'}$ with $k+p-r+1 \leqslant j' \leqslant p$ with one possible exception: S_{k+p-r} does not commute with $S_{k+p-r+1}$. These factors are both present if both $c_{p,k-1} = c_{p,k} = 0$. Now since $i = p$ is the first value that maximizes $\Phi_{i,k}$ we have

$$0 < \Phi_{p,k} - \Phi_{p-1,k} = c_{p,k-1} - c_{p-1,k} \tag{7.13}$$

by (7.8). Now $c_{p-1,k} \geqslant 0$ and so $c_{p,k-1} > 0$. Hence $\Omega'_p(D_p)$ does not involve S_{k+p-r}, proving the first identity in (7.12). On the other hand $d_{p,k}(f_k v) = d_{p,k}(v) + 1$ while $d_{p,j}(f_k v) = d_{p,j}(v)$ for all $j \neq k$. Therefore $c_{p,k}(f_k v) = c_{p,k}(v) + 1 > 0$ and so $S_{k+p-r-1}$ does not appear in $\Omega''_p(f_k D_p)$, proving the second identity in (7.12).

Now using (7.12) we may rearrange the products and write $\sigma^\dagger(v) = \{\sigma_1^\dagger(v)\sigma_2^\dagger(v)\sigma_3^\dagger(v)\}$ where

$$\sigma_1^\dagger(v) = \Omega_{r-1}(D_{r-1}) \cdots \Omega_{p+1}(D_{p+1})\Omega''_p(D_p(v)),$$

$$\sigma_2^\dagger(v) = \Omega_p'(D_p(v))\Omega_{p-1}(D_{p-1})\cdots\Omega_{r-k}(D_{r-k}),$$
$$\sigma_3^\dagger(v) = \Omega_{r-k-1}(D_{r-k-1})\cdots\Omega_1(D_1),$$

and similarly for $f_k v$. Here all factors $\Omega_i(D_i)$ with $i \neq p$ are the same for v and $f_k v$ so we omit the v from the notation except when $i = p$. Then we trivially have that $\sigma_3^\dagger(f_k v) = \sigma_3^\dagger(v)$ and will show that

$$\sigma_1^\dagger(f_k v) = \sigma_1^\dagger(v) \quad \text{or} \quad S_k \sigma_1^\dagger(f_k v) \tag{7.14}$$

and

$$\sigma_2^\dagger(f_k v) = \sigma_2^\dagger(v). \tag{7.15}$$

The lemma will follow upon demonstrating these two identities.

Let us prove (7.14). Since $c_{p,k}(f_k v) = c_{p,k}(v) + 1 > 0$ as shown above, we have that $\Omega_p''(D_p(f_k v)) = \Omega_p''(f_k D_p(v)) = \Omega_p''(D_p(v))$ unless $c_{p,k} = 0$. If this is true we are done, so we assume that $c_{p,k} = 0$. Then

$$\Omega_p''(D_p) = S_{k+p-r+1}\Omega_p''(f_k D_p).$$

Thus what we must show is that either

$$\Omega_{r-1}(D_{r-1})\cdots\Omega_{p+1}(D_{p+1})S_{k+p-r+1} = \begin{cases} S_k\Omega_{r-1}(D_{r-1})\cdots\Omega_{p+1}(D_{p+1}) & \text{or} \\ \Omega_{r-1}(D_{r-1})\cdots\Omega_{p+1}(D_{p+1}). \end{cases} \tag{7.16}$$

We will prove this, obtaining a series of inequalities along the way. First consider $\Omega_{p+1}(D_{p+1})S_{k+p-r+1}$. Let us argue that $\Omega_{p+1}(D_{p+1})$ involves $S_{k+p-r+1}$. Indeed, its presence is conditioned on $c_{p+1,k-1} = 0$. Now since the first value where $\Phi_{i,k}$ attains its maximum is at $i = p$, we have $0 \leqslant \Phi_{p,k} - \Phi_{p+1,k} = c_{p,k} - c_{p+1,k-1}$. Therefore $c_{p+1,k-1} \leqslant c_{p,k} = 0$, so $c_{p+1,k-1} = 0$. Thus $\Omega_{p+1}(D_{p+1})$ involves $S_{k+p-r+1}$ and $c_{p+1,k-1} = c_{p,k} = 0$. Now unless $c_{p+1,k} = 0$, the product $\Omega_{p+1}(D_{p+1})$ does not involve $S_{k+p-r+2}$ and so $\Omega_{p+1}(D_{p+1}) = \cdots S_{k+p-r+1}\cdots$, where the second ellipsis represents factors that all commute with $S_{k+p-r+1}$. Therefore since $S_{k+p-r+1}^2 = S_{k+p-r+1}$ we have $\Omega_{p+1}(D_{p+1})S_{k+p-r+1} = \Omega_{p+1}(D_{p+1})$, and (7.16) is proved. This means that we may assume that $c_{p+1,k} = 0$ and so $\Omega_{p+1}(D_{p+1}) = \cdots S_{k+p-r+1}S_{k+p-r+2}\cdots$ where again the second ellipsis represents factors that all commute with $S_{k+p-r+1}$. Now we use the braid relation and write

$$\Omega_{p+1}(D_{p+1})S_{k+p-r+1} = \cdots S_{k+p-r+1}S_{k+p-r+2}\cdots S_{k+p-r+1}$$
$$= \cdots S_{k+p-r+2}S_{k+p-r+1}S_{k+p-r+2}\cdots.$$

The first ellipsis represents factors that commute with $S_{k+p-r+2}$ and so we obtain

$$\Omega_{p+1}(D_{p+1})S_{k+p-r+1} = S_{k+p-r+2}\Omega_{p+1}(D_{p+1}).$$

We wish to repeat the process so we consider now $\Omega_{p+2}(D_{p+2})S_{k+p-r+2}$. To continue, we need to know that $c_{p+2,k-1} = 0$. Because the first value where $\Phi_{i,k}$ attains its maximum is at $i = p$, we have $0 \leqslant \Phi_{p,k} - \Phi_{p+2,k} = c_{p,k} - c_{p+1,k-1} + c_{p+1,k} - c_{p+2,k-1}$. Since we already have $c_{p,k} = c_{p+1,k-1} = c_{p+1,k} = 0$ we have $c_{p+2,k-1} \leqslant c_{p+1,k} = 0$ so $c_{p+2,k-1} = 0$ as required. Now the same argument as before produces either $\Omega_{p+2}(D_{p+2})S_{k+p-r+2} = \Omega_{p+2}(D_{p+2})$, in which case we are done, or

$$\Omega_{p+2}(D_{p+2})S_{k+p-r+2} = S_{k+p-r+2}\Omega_{p+1}(D_{p+1})$$

and the further equality $c_{p+2,k} = 0$. Repeating this argument gives a succession of identities which together imply (7.16) and (7.14).

Now let us prove (7.15). We recall that $D_p(f_k v) = f_k D_p(v)$ differs from $D_p(v)$ in replacing $d_{p,k}$ by $d_{p,k} + 1$. This can change only the last factor in $\Omega'_p(D_p)$, and this only if $d_{p,k} = d_{p,k-1} - 1$. Therefore we may assume that $c_{p,k-1} = 1$ and $\Omega'_p(D_p(f_k v)) = \Omega'(D_p(v))S_{k+p-r}$. Therefore what we must prove is that

$$S_{k+p-r}\Omega_{p-1}(D_{p-1})\cdots\Omega_{r-k}(D_{r-k}) = \Omega_{p-1}(D_{p-1})\cdots\Omega_{r-k}(D_{r-k}). \tag{7.17}$$

Thus consider $S_{k+p-r}\Omega_{p-1}(D_{p-1})$. We have $c_{p-1,k} < c_{p,k-1} = 1$ by (7.13), and so $c_{p-1,k} = 0$. This means that $\Omega_{p-1}(D_{p-1})$ has S_{k+p-r} as a factor, and unless it also has $S_{k+p-r-1}$ as a factor, we obtain $S_{k+p-r}\Omega_{p-1}(D_{p-1}) = \Omega_{p-1}(D_{p-1})$, which implies (7.15). Therefore we may assume that $\Omega_{p-1}(D_{p-1})$ has $S_{k+p-r-1}$ as a factor, which means that $c_{p-1,k-1} = 0$, which we now assume. Now we use $S_{k+p-r}\Omega_{p-1}(D_{p-1}) = S_{k+p-r}\cdots S_{k+p-r-1}S_{k+p-r}\cdots$ where the first ellipsis represents factors that commute with S_{k+p-r} and the second ellipsis represents factors that commute with $S_{k+p-r-1}$. Using the braid relation we obtain

$$S_{k+p-r}\Omega_{p-1}(D_{p-1}) = \Omega_{p-1}(D_{p-1})S_{k+p-r-1}.$$

We repeat the process. The next step is to prove that either

$$S_{k+p-r-1}\Omega_{p-2}(D_{p-2}) = \Omega_{p-2}(D_{p-2}) \qquad \text{or} \qquad \Omega_{p-2}(D_{p-2})S_{k+p-r-2}.$$

If $S_{k+p-r-1}\Omega_{p-2}(D_{p-2}) = \Omega_{p-2}(D_{p-2})$ then (7.15) follows and we may stop; otherwise we will prove the second identity together with the equation $c_{p-2,k} = c_{p-2,k-1} = 0$ that will be needed for subsequent steps. Since $i = p$ is the first value to maximize $\Phi_{i,k}$ we have, using (7.8)

$$0 < \Phi_{p,k} - \Phi_{p-2,k} = \Phi_{p,k} - \Phi_{p-1,k} + \Phi_{p-1,k} - \Phi_{p-2,k} = c_{p,k-1} - c_{p-1,k} + c_{p-1,k-1} - c_{p-2,k}.$$

We already have $c_{p,k-1} = 1$ while $c_{p-1,k} = c_{p-1,k-1} = 0$, so $c_{p-2,k} = 0$. This means that $\Omega_{p-2}(D_{p-2})$ has a factor $S_{k+p-r-1}$. Unless it also has a factor $S_{k+p-r-2}$ we

have $S_{k+p-r-1}\Omega_{p-2}(D_{p-2}) = \Omega_{p-2}(D_{p-2})$ and we are done. If it does have the factor $S_{k+p-r-2}$ then we have $c_{p-2,k-1} = 0$ and $S_{k+p-r-1}\Omega_{p-2}(D_{p-2}) = \Omega_{p-2}(D_{p-2})S_{k+p-r-2}$ follows from the braid relation. Continuing this way, we obtain a sequence of identities $c_{p-a,k} = 0$ and

$$S_{k+p-r+1-a}\Omega_{p-a}(D_{p-a}) = \Omega_{p-a}(D_{p-a}) \qquad \text{or} \qquad \Omega_{p-a}(D_{p-a})S_{p+k-r-a}.$$

If first alternative is true we may stop, since then (7.17) is proved and we are done. Otherwise if the second equality is true we have also $c_{p-a,k-1} = 0$, which is used to prove $c_{p-a-1,k} = 0$ by an argument as above based on (7.8) and move to the next stage. Finally, with $c_{r-k,k} = 0$, the last identity to be proved is

$$S_1\Omega_{r-k}(D_{r-k}) = \Omega_{r-k}(D_{r-k}),$$

and this time there is no second alternative. This is true since then the first factor of $\Omega_{r-k}(D_{r-k})$ is S_1, and $S_1^2 = S_1$. Now (7.17) is proved, establishing (7.15). □

Lemma 7.6. *Let $w \in W$. Then*

$$\mathcal{B}_\infty(w^{-1}) \subseteq \{v \in \mathcal{B}_\infty \mid w_0\sigma(v^\star) \leqslant w\} \tag{7.18}$$

and

$$\mathcal{B}_\infty(w) \subseteq \{v \in \mathcal{B}_\infty \mid w_0\sigma(v) \leqslant w\}. \tag{7.19}$$

We will improve the inclusions in this Lemma later in Theorem 8.1 to equalities, taking into account the additional information we have from Theorem 4.4.

Proof of Lemma 7.6. By [32] or [18] Theorem 14.17, the $\star$-involution takes $\mathcal{B}_\infty(w^{-1})$ to $\mathcal{B}_\infty(w)$. Thus (7.18) and (7.19) are equivalent. Using Lemma 7.4 and the fact that the inverse map on W preserves the Bruhat order, (7.18) is also equivalent to

$$\mathcal{B}_\infty(w) \subseteq \{v \in \mathcal{B}_\infty \mid \sigma^\dagger(v)w_0 \leqslant w\}, \tag{7.20}$$

which we will now prove by induction on $\ell(w)$. If $w = 1$ then $\mathcal{B}_\infty(1) = \{u_0\}$, where u_0 is the highest weight vector in $\mathcal{B}_\infty$. For $v = u_0$ all the conditions $c_{i,r-1+j-1} = 0$ are satisfied in (7.9) and it follows that $\sigma^\dagger(u_0) = w_0$, so (7.20) is satisfied in this case. Now assume that (7.20) is true for w; we show that if s_i is a simple reflection and $s_iw > w$ then it is also true for s_iw. Now, by Theorem 5.1 (i) for $\mathcal{B} = \mathcal{B}_\infty$, if $v \in \mathcal{B}_\infty(s_iw)$ then there is a $v_1 \in \mathcal{B}_\infty(w)$ such that v and v_1 lie in the same root string. Note that Lemma 7.5 implies that if v, v_1 lie in the same i-string then either $\sigma^\dagger(v_1) = \sigma^\dagger(v)$ or $\sigma^\dagger(v_1) = s_i\sigma^\dagger(v)$. Then $\sigma^\dagger(v_1)w_0 \leqslant w$ by induction, and $\sigma^\dagger(v)w_0 = \sigma^\dagger(v_1)w_0$ or $s_i\sigma^\dagger(v_1)w_0$; in either case $\sigma^\dagger(v)w_0 \leqslant s_iw$. □

8. Proof of Theorem 5.5

In this section we will prove Theorem 5.5 and its $\mathcal{B}_\infty$ analogue.

Proof of Theorem 5.5. We consider the preimage in $\mathcal{B}_\lambda$ of both sides of the identity in Lemma 7.6 under the map $\psi_\lambda : \mathcal{B}_\lambda \to \mathcal{B}_\infty$ defined in Section 7 and we obtain the inclusion of sets

$$\mathcal{B}_\lambda(w) \subseteq \{v \in \mathcal{B}_\lambda \mid w_0\sigma(v) \leqslant w\} = \bigcup_{y \leqslant w} \{v \in \mathcal{B}_\lambda \mid w_0\sigma(v) = y\}. \tag{8.1}$$

We claim that, in fact, these sets are equal, which would give us (5.1). We caution the reader that the Kashiwara involution $\star$ (which is not a crystal isomorphism) does not preserve $\mathcal{B}_\lambda$ embedded in the crystal via ψ_λ. What is true is that it maps $\mathcal{B}_\infty(w)$ into $\mathcal{B}_\infty(w^{-1})$, and the preimage of $\mathcal{B}_\infty(w)$ in $\mathcal{B}_\lambda$ is $\mathcal{B}_\lambda(w)$. That is all that is needed for (8.1).

Let X and Y be the two subsets of $\mathcal{B}_\lambda$ on the left- and right-hand sides of (8.1). We have just shown that $X \subseteq Y$. Now, on the one hand, we have from Theorem 5.1 (iii) that

$$\sum_{\mathfrak{T} \in X} \mathbf{z}^{\mathrm{wt}(\mathfrak{T})} = \partial_w \mathbf{z}^\lambda . \tag{8.2}$$

On the other hand, using the bijection between the crystal $\mathcal{B}_\lambda$ and the ensemble of states $\mathfrak{S}_{\mathbf{z},\lambda}$ together with Theorem 6.1, we have that

$$\sum_{\mathfrak{T} \in Y} \mathbf{z}^{\mathrm{wt}(\mathfrak{T})} := \sum_{y \leqslant w} \sum_{\substack{v \in \mathcal{B}_\lambda \\ w_0\sigma(v)=y}} \mathbf{z}^{\mathrm{wt}(v)} = \sum_{y \leqslant w} \sum_{s \in \mathfrak{S}_{\mathbf{z},\lambda,y}} \mathbf{z}^{\mathrm{wt}(\mathfrak{T}(s)')} .$$

The Schützenberger involution satisfies the property that $\mathrm{wt}(\mathfrak{T}') = w_0 \, \mathrm{wt}(\mathfrak{T})$. Using this, then (i) of Proposition 3.2 and then Theorem 4.4 we get that

$$\sum_{s \in \mathfrak{S}_{\mathbf{z},\lambda,y}} \mathbf{z}^{\mathrm{wt}(\mathfrak{T}(s)')} = \sum_{s \in \mathfrak{S}_{\mathbf{z},\lambda,y}} \mathbf{z}^{w_0 \, \mathrm{wt}(\mathfrak{T}(s))} = \mathbf{z}^{-\rho} Z(\mathfrak{S}_{\mathbf{z},\lambda,y}) = \partial_y^\circ \mathbf{z}^\lambda .$$

Finally by Theorem 2.1 and comparing with (8.2), it follows that

$$\sum_{\mathfrak{T} \in Y} \mathbf{z}^{\mathrm{wt}(\mathfrak{T})} = \sum_{y \leqslant w} \partial_y^\circ \mathbf{z}^\lambda = \partial_w \mathbf{z}^\lambda = \sum_{\mathfrak{T} \in X} \mathbf{z}^{\mathrm{wt}(\mathfrak{T})}. \tag{8.3}$$

Setting $\mathbf{z} = 1_T$ in the above equality shows that X and Y have the same cardinality. Therefore $X = Y$.

The assertion that $w_0\sigma(v) = w$ implies that w is the longest element of its coset in W/W_λ is Corollary 6.3. □

Now that Theorem 5.5 is proved, we have an analogous characterization of Demazure crystals and Demazure atoms in $\mathcal{B}_\infty$.

Theorem 8.1. *For any $w \in W$,*

$$\mathcal{B}_\infty(w) = \{v \in \mathcal{B}_\infty \mid \sigma^\dagger(v)w_0 \leqslant w\} = \{v \in \mathcal{B}_\infty \mid w_0\sigma(v) \leqslant w\}. \tag{8.4}$$

The map σ satisfies

$$w_0\sigma(v)w_0 = \sigma^\dagger(v) = \sigma(v^\star)^{-1}. \tag{8.5}$$

Proof. The identities

$$\mathcal{B}_\lambda(w) = \{v \in \mathcal{B}_\lambda \mid \sigma^\dagger(v)w_0 \leqslant w\} = \{v \in \mathcal{B}_\lambda \mid w_0\sigma(v) \leqslant w\}$$

have been proved for the finite crystal $\mathcal{B}_\lambda$, and since the images of ψ_λ exhaust $\mathcal{B}_\infty$, (8.4) follows. The identity (8.5) follows using Lemma 7.4. □

Now the Demazure atoms in $\mathcal{B}_\infty$ may be defined as

$$\mathcal{B}_\infty^\circ(w) = \{v \in \mathcal{B}_\infty \mid \sigma^\dagger(v)w_0 = w\} = \{v \in \mathcal{B}_\infty \mid w_0\sigma(v) = w\}. \tag{8.6}$$

Corollary 8.2. *The subsets $\mathcal{B}_\infty^\circ(w)$ are a family of crystal Demazure atoms for $\mathcal{B}_\infty$.*

Proof. These are obviously a family of disjoint subsets of $\mathcal{B}_\infty$ and by Theorem 8.1 they satisfy the characterizing identity (5.1). □

9. Proof of the algorithms for computing Lascoux-Schützenberger keys

We now prove the algorithms from Subsection 1.1. For the first algorithm, given any tableau $T \in \mathcal{B}_\lambda$, we compute $\sigma(T')$ by means of the definition (5.11). Thus we consider $\text{string}_{\mathbf{i}'}^{(e)}(T') = \text{string}_{\mathbf{i}}^{(f)}(T) = (b_1, b_2, \cdots)$, where the Gelfand-Tsetlin pattern of T is the array (a_{ij}) and the b_i are given by the formula (6.2). Then

$$
\begin{aligned}
b_1 = 0 &\quad\Longleftrightarrow\quad a_{r,r} = a_{r-1,r}, \\
b_2 = b_3 &\quad\Longleftrightarrow\quad a_{r-1,r-1} = a_{r-2,r-1}, \\
b_3 = 0 &\quad\Longleftrightarrow\quad a_{r-1,r} = a_{r-2,r}, \\
&\qquad\qquad\vdots
\end{aligned}
$$

and so forth. This means that the circled entries in (1.4) are the same as in (5.10). Therefore the first algorithm follows from Theorem 5.5.

We may now prove Algorithm 2. The idea is to deduce it from Algorithm 1 (which is already proved) for the crystal $\mathcal{B}_{-w_0\lambda}$. Now $-w_0\lambda = (-\lambda_r, \cdots, -\lambda_1)$ is not a partition (since its entries may be negative) but it is a dominant weight. Fortunately the facts that we need, particularly the map to Gelfand-Tsetlin patterns and Algorithm 1, may be extended to crystals $\mathcal{B}_\lambda$ where λ is a dominant weight by the following considerations.

If $\lambda = (\lambda_1, \cdots, \lambda_r)$ a dominant weight (that is, $\lambda_1 \geqslant \cdots \geqslant \lambda_r$ but the entries may be negative) then for sufficiently large N, $\lambda + N^r = (\lambda_1 + N, \cdots, \lambda_r + N)$ is a partition and $\mathcal{B}_{\lambda+(N^r)}$ is a crystal of tableaux. To put this into context, $\mathcal{B}_\lambda$ is the crystal of the representation π_λ of $\mathrm{GL}(r)$ with highest weight λ, and $\mathcal{B}_{\lambda+(N^r)}$ is the crystal of $\det^N \otimes \pi_\lambda$. The crystal graph of $\mathcal{B}_{\lambda+(N^r)}$ is isomorphic to that of $\mathcal{B}_\lambda$ and we may transfer results such as Theorem 5.5 from $\mathcal{B}_{\lambda+(N^r)}$ to $\mathcal{B}_\lambda$.

In particular let $\mathfrak{P}_\lambda$ be the space of Gelfand-Tsetlin patterns with top row λ. Let $\Gamma : \mathcal{B}_\lambda \longrightarrow \mathfrak{P}_\lambda$ be the map defined in the introduction for λ a partition. If λ is a dominant weight, then $\Gamma : \mathcal{B}_\lambda \longrightarrow \mathfrak{P}_\lambda$ may be similarly defined; for if $v \in \mathcal{B}_\lambda$ and T is the corresponding element of $\mathcal{B}_{\lambda+(N^r)}$, then $\Gamma(T)$ is defined and we define $\Gamma(v)$ to be the Gelfand-Tsetlin pattern obtained from $\Gamma(T)$ by subtracting N from every element of $\Gamma(T)$. The map $\sigma : \mathcal{B}_\lambda \longrightarrow W$ is also defined and Algorithm 1 is valid.

Now there are maps $\alpha_1, \alpha_2 : \mathfrak{P}_\lambda \longrightarrow W$ corresponding to Algorithm 1 and Algorithm 2 of the introduction. Thus if $a = (a_{ij})$ is a Gelfand-Tsetlin pattern, then for each (i, j) with $a_{i,j} = a_{i-1,j}$ we circle the corresponding entry in (1.4) and $\alpha_1(a)$ will be the nondescending product of the circled reflection in order from bottom to top, right to left; and similarly to compute $\alpha_2(a)$ we circle the entries of (1.5) when $a_{i,j} = a_{i-1,j-1}$ and take the nondescending product in order from bottom to top, left to right.

There is an operation $-\mathrm{rev}$ on Gelfand-Tsetlin patterns that maps $\mathfrak{P}_\lambda$ to $\mathfrak{P}_{-w_0\lambda}$ that negates the entries in a pattern a and mirror-reflects them from left to right, so if $r = 3$

$$-\mathrm{rev}\left(\left\{\begin{matrix} \lambda_1 & & \lambda_2 & & \lambda_3 \\ & a & & b & \\ & & c & & \end{matrix}\right\}\right) = \left\{\begin{matrix} -\lambda_3 & & -\lambda_2 & & -\lambda_1 \\ & -b & & -a & \\ & & -c & & \end{matrix}\right\}.$$

As further discussed in [13], there is a map $\phi_\lambda : \mathcal{B}_\lambda \longrightarrow \mathcal{B}_{-w_0\lambda}$ that maps the highest weight element to the highest weight element and has the effect that $\phi_\lambda(e_i v) = e_{i'}\phi_\lambda(v)$, where we recall that $i' = r - i$.

Proposition 9.1. *For all $T \in \mathcal{B}_\lambda$*

$$\sigma(\phi_\lambda(T)) = w_0\sigma(T)w_0^{-1}. \tag{9.1}$$

Proof. Note that $w \mapsto w_0 w w_0^{-1}$ is the automorphism of W that sends the simple reflection s_i to $s_{i'}$. So by the definition of the Demazure crystals it is clear that $\phi_\lambda \mathcal{B}_\lambda(w) = \mathcal{B}_{-w_0\lambda}(w_0 w w_0^{-1})$. Hence $\phi_\lambda(\mathcal{B}_\lambda^\circ(w)) = \mathcal{B}_{-w_0\lambda}^\circ(w_0 w w_0^{-1})$. By Theorem 5.5, we may characterize $\sigma(T)$ as the shortest Weyl group element such that $T \in \mathcal{B}_\lambda^\circ(w_0\sigma(T))$. Equation (9.1) follows. $\square$

The map ϕ_λ intertwines the Schützenberger-Lusztig involutions $v \mapsto v'$ on $\mathcal{B}_\lambda$ and $\mathcal{B}_{-w_0\lambda}$. We will denote $\phi'_\lambda(v) = \phi_\lambda(v') = \phi_\lambda(v)'$. Let $\tau : W \longrightarrow W$ be conjugation by w_0. We have a commutative diagram

$$
\begin{array}{ccc}
\mathcal{B}_\lambda & \xrightarrow{\;\;\phi'_\lambda\;\;} & \mathcal{B}_{-w_0\lambda} \\
\downarrow{\scriptstyle\Gamma} & & \downarrow{\scriptstyle\Gamma} \\
\mathfrak{P}_\lambda & \xrightarrow{\;-\mathrm{rev}\;} & \mathfrak{P}_{-w_0\lambda} \\
\downarrow{\scriptstyle\alpha_2} & & \downarrow{\scriptstyle\alpha_1} \\
W & \xrightarrow{\;\;\tau\;\;} & W
\end{array}
$$

Indeed, the top square commutes by (2.12) of [13], which is proved there using the description of the Schützenberger involution on Gelfand-Tsetlin patterns in [35]. The commutativity of the bottom square is clear from the definitions of α_1 and α_2, bearing in mind that $w_0 s_i w_0^{-1} = s_{i'}$ when circling (1.4) and (1.5).

We may now prove the second algorithm. If $T \in \mathcal{B}_\lambda$, the commutative diagram shows that

$$
w_0 \alpha_2(\Gamma(T)) w_0^{-1} = \alpha_1(\Gamma(\phi_\lambda(T)')) = \sigma(\phi_\lambda(T)) = w_0 \sigma(T) w_0^{-1}
$$

where the second step is by applying Algorithm 1 to $\phi_\lambda(T)' \in \mathcal{B}_{-w_0\lambda}$ and the last step is by (9.1). Therefore $\sigma(T) = \alpha_2(\Gamma(T))$, which is Algorithm 2.

References

[1] Y. Akutsu, T. Deguchi, T. Ohtsuki, Invariants of colored links, J. Knot Theory Ramif. 1 (2) (1992) 161–184.

[2] S. Assaf, A. Schilling, A Demazure crystal construction for Schubert polynomials, Algebraic Combin. 1 (2) (2017) 225–247, arXiv:1705.09649.

[3] J.-C. Aval, Keys and alternating sign matrices, Sémin. Lothar. Comb. 59 (2007/10) B59f, 13.

[4] R.J. Baxter, Exactly Solved Models in Statistical Mechanics, Academic Press Inc. [Harcourt Brace Jovanovich Publishers], London, 1982.

[5] A. Berenstein, A. Zelevinsky, Canonical bases for the quantum group of type A_r and piecewise-linear combinatorics, Duke Math. J. 82 (3) (1996) 473–502.

[6] I.N. Bernstein, I.M. Gel'fand, S.I. Gel'fand, Schubert cells, and the cohomology of the spaces G/P, Usp. Mat. Nauk 28 (3(171)) (1973) 3–26.

[7] A. Borodin, On a family of symmetric rational functions, Adv. Math. 306 (2017) 973–1018.

[8] A. Borodin, A. Bufetov, M. Wheeler, Between the stochastic six vertex model and Hall-Littlewood processes, arXiv:1611.09486, 2016.

[9] A. Borodin, M. Wheeler, Coloured stochastic vertex models and their spectral theory, arXiv:1808.01866, 2018.

[10] B. Brubaker, V. Buciumas, D. Bump, A Yang-Baxter equation for metaplectic ice, Commun. Number Theory Phys. 13 (1) (2019) 101–148.

[11] B. Brubaker, V. Buciumas, D. Bump, H. Gustafsson, Colored vertex models and Iwahori Whittaker functions, arXiv:1906.04140, 2019.

[12] B. Brubaker, D. Bump, S. Friedberg, Schur polynomials and the Yang-Baxter equation, Commun. Math. Phys. 308 (2) (2011) 281–301.

[13] B. Brubaker, D. Bump, S. Friedberg, Weyl Group Multiple Dirichlet Series: Type A Combinatorial Theory, Annals of Mathematics Studies, vol. 175, Princeton University Press, Princeton, NJ, 2011.

[14] B. Brubaker, C. Frechette, A. Hardt, E. Tibor, K. Weber, Frozen pipes: lattice models for Grothendieck polynomials, arXiv:2007.04310, 2020.

[15] V. Buciumas, T. Scrimshaw, Double Grothendieck polynomials and colored lattice models, arXiv:2007.04533, 2020.

[16] V. Buciumas, T. Scrimshaw, K. Weber, Colored five-vertex models and Lascoux polynomials and atoms, arXiv:1908.07364, 2019.

[17] D. Bump, Lie Groups, second edition, Graduate Texts in Mathematics, vol. 225, Springer, New York, 2013.

[18] D. Bump, A. Schilling, Crystal Bases, Representations and Combinatorics, World Scientific Publishing Co. Pte. Ltd., Hackensack, NJ, 2017.

[19] I. Corwin, L. Petrov, Stochastic higher spin vertex models on the line, Commun. Math. Phys. 343 (2) (2016) 651–700.

[20] M. Demazure, Désingularisation des variétés de Schubert généralisées, Ann. Sci. Éc. Norm. Supér. (4) 7 (1974) 53–88, Collection of articles dedicated to Henri Cartan on the occasion of his 70th birthday, I.

[21] V.V. Deodhar, Some characterizations of Bruhat ordering on a Coxeter group and determination of the relative Möbius function, Invent. Math. 39 (2) (1977) 187–198.

[22] C. Ehresmann, Sur la topologie de certains espaces homogènes, Ann. of Math. (2) 35 (2) (1934) 396–443.

[23] O. Foda, M. Wheeler, Colour-independent partition functions in coloured vertex models, Nucl. Phys. B 871 (2) (2013) 330–361.

[24] S. Fomin, A.N. Kirillov, The Yang-Baxter equation, symmetric functions, and Schubert polynomials, in: Proceedings of the 5th Conference on Formal Power Series and Algebraic Combinatorics, Florence, 1993, vol. 153, 1996, pp. 123–143.

[25] V. Gorbounov, C. Korff, Quantum integrability and generalised quantum Schubert calculus, Adv. Math. 313 (2017) 282–356.

[26] V. Gorbounov, C. Korff, C. Stroppel, Yang-Baxter algebras as convolution algebras: the Grassmannian case, arXiv:1802.09497, 2018.

[27] A.M. Hamel, R.C. King, Bijective proofs of shifted tableau and alternating sign matrix identities, J. Algebraic Comb. 25 (4) (2007) 417–458.

[28] P. Hersh, C. Lenart, From the weak Bruhat order to crystal posets, Math. Z. 286 (3–4) (2017) 1435–1464.

[29] N. Jacon, C. Lecouvey, Keys and Demazure crystals for Kac-Moody algebras, arXiv:1909.09520, 2019.

[30] M. Jimbo, T. Miwa, Algebraic Analysis of Solvable Lattice Models, CBMS Regional Conference Series in Mathematics, vol. 85, American Mathematical Society, Providence, RI, 1995, Published for the Conference Board of the Mathematical Sciences, Washington, DC.

[31] A. Joseph, Consequences of the Littelmann path theory for the structure of the Kashiwara $B(\infty)$ crystal, in: Highlights in Lie Algebraic Methods, in: Progr. Math., vol. 295, Birkhäuser/Springer, New York, 2012, pp. 25–64.

[32] M. Kashiwara, The crystal base and Littelmann's refined Demazure character formula, Duke Math. J. 71 (3) (1993) 839–858.

[33] M. Kashiwara, Bases cristallines des groupes quantiques, Cours Spécialisés [Specialized Courses], vol. 9, Société Mathématique de France, Paris, 2002, Edited by Charles Cochet.

[34] M. Kashiwara, T. Nakashima, Crystal graphs for representations of the q-analogue of classical Lie algebras, J. Algebra 165 (2) (1994) 295–345.

[35] A.N. Kirillov, A.D. Berenstein, Groups generated by involutions, Gelfand-Tsetlin patterns, and combinatorics of Young tableaux, Algebra Anal. 7 (1) (1995) 92–152.

[36] A. Knutson, E. Miller, Gröbner geometry of Schubert polynomials, Ann. of Math. (2) 161 (3) (2005) 1245–1318.

[37] A. Knutson, P. Zinn-Justin, Schubert puzzles and integrability I: invariant trilinear forms, arXiv:1706.10019, 2017.

[38] V.E. Korepin, N.M. Bogoliubov, A.G. Izergin, Quantum Inverse Scattering Method and Correlation Functions, Cambridge Monographs on Mathematical Physics, Cambridge University Press, Cambridge, 1993.

[39] G. Kuperberg, Another proof of the alternating-sign matrix conjecture, Int. Math. Res. Not. 3 (1996) 139–150.

[40] A. Lascoux, The 6 vertex model and Schubert polynomials, SIGMA Symmetry Integrability Geom. Methods Appl. 3 (2007) 029, 12.

[41] A. Lascoux, B. Leclerc, J.-Y. Thibon, Flag varieties and the Yang-Baxter equation, Lett. Math. Phys. 40 (1) (1997) 75–90.

[42] A. Lascoux, M.-P. Schützenberger, Keys & standard bases, in: Invariant Theory and Tableaux, Minneapolis, MN, 1988, in: IMA Vol. Math. Appl., vol. 19, Springer, New York, 1990, pp. 125–144.

[43] C. Lenart, A unified approach to combinatorial formulas for Schubert polynomials, J. Algebraic Comb. 20 (3) (2004) 263–299.

[44] P. Littelmann, Crystal graphs and Young tableaux, J. Algebra 175 (1) (1995) 65–87.

[45] P. Littelmann, Cones, crystals, and patterns, Transform. Groups 3 (2) (1998) 145–179.

[46] S. Mason, A decomposition of Schur functions and an analogue of the Robinson-Schensted-Knuth algorithm, Sémin. Lothar. Comb. 60 (2006) B57e, arXiv:math/0604430.

[47] S. Mason, An explicit construction of type A Demazure atoms, J. Algebraic Comb. 29 (3) (2009) 295–313.

[48] R.A. Proctor, M.J. Willis, Semistandard tableaux for Demazure characters (key polynomials) and their atoms, Eur. J. Comb. 43 (2015) 172–184.

[49] V. Reiner, M. Shimozono, Key polynomials and a flagged Littlewood-Richardson rule, J. Comb. Theory, Ser. A 70 (1) (1995) 107–143.

[50] J.M. Santos, Symplectic keys and Demazure atoms in type C, arXiv:1910.14115, 2019.

[51] J.W. Seaborn III, Combinatorial interpretation of the Kumar-Peterson limit for $sl_n(\mathbb{C})$ Demazure characters and Gelfand pattern description of $sl_n(\mathbb{C})$ Demazure characters, Thesis (PhD), The University of North Carolina at Chapel Hill, ProQuest LLC, Ann Arbor, MI, 2014.

[52] J.R. Stembridge, A short derivation of the Möbius function for the Bruhat order, J. Algebraic Comb. 25 (2) (2007) 141–148.

[53] T. Tokuyama, A generating function of strict Gelfand patterns and some formulas on characters of general linear groups, J. Math. Soc. Jpn. 40 (4) (1988) 671–685.

[54] D.-N. Verma, Möbius inversion for the Bruhat ordering on a Weyl group, Ann. Sci. Éc. Norm. Supér. (4) 4 (1971) 393–398.

[55] M. Wheeler, P. Zinn-Justin, Littlewood–Richardson coefficients for Grothendieck polynomials from integrability, J. Reine Angew. Math. 757 (2019) 159–195.

[56] M.J. Willis, New Descriptions of Demazure Tableaux and Right Keys, with Applications to Convexity, Thesis (PhD), The University of North Carolina at Chapel Hill, ProQuest LLC, Ann Arbor, MI, 2012.

[57] M.J. Willis, A direct way to find the right key of a semistandard Young tableau, Ann. Comb. 17 (2) (2013) 393–400.

[58] M.J. Willis, Relating the right key to the type A filling map and minimal defining chains, Discrete Math. 339 (10) (2016) 2410–2416.